การประเมินอิทธิพลของอนุภาคทองคำระดับนาโนเมตรต่อการเปลี่ยนแปลงความชราระดับเซลล์ใน
เซลล์พรีอะดิโพไซต์ (3T3-L1) และไฟโบรบลาส์ (NIH 3T3) เมื่อถูกกระตุ้นด้วยไฮโดรเจนเปอร์ออกไซด์

นางสาวเฉลิมศรี ฉายัษฐิต

วิทยานิพนธ์นี้เป็นส่วนหนึ่งของการศึกษาตามหลักสูตรปริญญาวิทยาศาสตรมหาบัณฑิต
สาขาวิชาวิทยาศาสตร์การแพทย์
คณะแพทยศาสตร์ จุฬาลงกรณ์มหาวิทยาลัย
ปีการศึกษา 2558

Evaluation of gold nanoparticles effect on cellular senescence change in preadipocyte (3T3-L1) and fibroblast (NIH 3T3) cell lines induced with hydrogen peroxide

Miss Chalermsri Chayutsatid

A Thesis Submitted in Partial Fulfillment of the Requirements
for the Degree of Master of Science Program in Medical Science
Faculty of Medicine
Chulalongkorn University
Academic Year 2015

Thesis Title	Evaluation of gold nanoparticles effect on cellular senescence change in preadipocyte (3T3-L1) and fibroblast (NIH 3T3) cell lines induced with hydrogen peroxide
By	Miss Chalermsri Chayutsatid
Field of Study	Medical Science
Thesis Advisor	Assistant Professor Amornpun Sereemaspun, M.D., Ph.D.
Thesis Co-Advisor	Dr.Narisorn Kongruttanachok

Accepted by the Faculty of Medicine, Chulalongkorn University in Partial Fulfillment of the Requirements for the Master's Degree

.....Dean of the Faculty of Medicine

(ProfessorSuttipong Wacharasindhu, M.D., Ph.D.)

THESIS COMMITTEE

.....Chairman

(ProfessorVilai Chentanez, M.D., Ph.D.)

.....Thesis Advisor

(Assistant Professor Amornpun Sereemaspun, M.D., Ph.D.)

.....Thesis Co-Advisor

(Dr.Narisorn Kongruttanachok)

.....Examiner

(Associate ProfessorPadet Siriyasatien, M.D., Ph.D)

.....Examiner

(Dr.Depicha Jindatip)

.....External Examiner

(Dr.Rujira Wanotayan)

เฉลิมศรี ฉายัษฐิต : การประเมินอิทธิพลของอนุภาคทองคำระดับนาโนเมตรต่อการเปลี่ยนแปลงความชราระดับเซลล์ในเซลล์พรีอะดิโพไซต์ (3T3-L1) และไฟโบรบลาส์ (NIH 3T3) เมื่อถูกกระตุ้นด้วยไฮโดรเจนเปอร์ออกไซด์ (Evaluation of gold nanoparticles effect on cellular senescence change in preadipocyte (3T3-L1) and fibroblast (NIH 3T3) cell lines induced with hydrogen peroxide) อ.ที่ปรึกษาวิทยานิพนธ์หลัก: ผศ. ดร. นพ.อมรพันธุ์ เสรีมาศพันธุ์, อ.ที่ปรึกษาวิทยานิพนธ์ร่วม: ดร.นริศร คงรัตนโชค, 63 หน้า.

ปัจจุบันมีการนำอนุภาคทองคำระดับนาโนเมตรมาประยุกต์ใช้ในงานหลากหลายสาขา เนื่องจากอนุภาคทองคำระดับนาโนเมตรมีคุณสมบัติพิเศษเฉพาะตัวและมีความเสถียรสูงซึ่งแตกต่างจาก อนุภาคระดับนาโนเมตรชนิดอื่น โดยเฉพาะในอุตสาหกรรมความงามมีการนำอนุภาคทองคำระดับนาโนเมตรมาใช้เป็นตัวนำส่งสารออกฤทธิ์เข้าสู่เซลล์ผิวหนัง เช่น เวชสำอาง ครีมบำรุงผิว ครีมกันแดด ผลิตภัณฑ์ต่อต้านริ้วรอยและการเสื่อมสภาพของเซลล์ เป็นต้น ถึงแม้ว่ามีหลายงานวิจัยที่ผ่านมาได้กล่าวถึงประโยชน์ของอนุภาคทองคำระดับนาโนเมตรในด้านช่วยชะลอเซลล์ชรา แต่มีงานวิจัยที่กล่าวถึงความเป็นพิษและการเร่งให้เซลล์ชราของของอนุภาคทองคำระดับนาโนเมตรเช่นกัน งานวิจัยนี้มีวัตถุประสงค์เพื่อประเมินอิทธิพลของอนุภาคทองคำระดับนาโนเมตรต่อการเปลี่ยนแปลงความชราระดับเซลล์ในเซลล์เริ่มต้นของเซลล์ไขมันและไฟโบรบลาสต์ โดยทำการทดสอบอิทธิพลของอนุภาคทองคำระดับนาโนเมตรกับความเป็นพิษต่อเซลล์ ลักษณะทางฟีโนไทป์ของเซลล์ชรา การเกิดอนุมูลอิสระภายในเซลล์ และกลไกความชราระดับเซลล์ซึ่งตรวจสอบการแสดงออกของยีนที่เกี่ยวข้องโดยวิธี RT-qPCR การทดลองนี้ใช้ไฮโดรเจนเปอร์ออกไซด์กระตุ้นให้เซลล์ชราและใช้อนุภาคทองคำระดับนาโนเมตรที่มีขนาดและความเข้มข้นแตกต่างกันในการทดลอง ผลการศึกษาพบว่า อนุภาคทองคำระดับนาโนเมตรขนาด 10 นาโมเมตร ความเข้มข้น 50 ppm มีความเป็นพิษต่อเซลล์ทั้งสองชนิด อนุภาคทองคำระดับนาโนเมตรขนาด 10 และ 20 นาโมเมตร สามารถป้องกันการเกิดลักษณะทางฟีโนไทป์ของเซลล์ชราเฉพาะในเซลล์เริ่มต้นของเซลล์ไขมันเท่านั้น อนุภาคทองคำระดับนาโนเมตรขนาด 10 และ 20 นาโมเมตร ไม่กระตุ้นให้เกิดอนุมูลอิสระภายในเซลล์ทั้งสองชนิดซึ่งแสดงว่าเซลล์ตอบสนองต่อความชราแบบไม่ขึ้นกับการเกิดอนุมูลอิสระภายในเซลล์ นอกจากนี้อนุภาคทองคำระดับนาโนเมตรขนาด 10 และ 20 นาโมเมตร ช่วยเพิ่มการแสดงออกของยีนเซอร์ทูอินวันและทูเมอร์ซัพเพรสเซอร์แต่ลดการแสดงออกของยีนซีอีบีพีแอลฟ่าและพีพาร์แกรมม่าเฉพาะในเซลล์เริ่มต้นของเซลล์ไขมัน

สาขาวิชา วิทยาศาสตร์การแพทย์ ลายมือชื่อนิสิต .....

ปีการศึกษา 2558 ลายมือชื่อ อ.ที่ปรึกษาหลัก .....

ลายมือชื่อ อ.ที่ปรึกษาร่วม .....

5674018530 : MAJOR MEDICAL SCIENCE
KEYWORDS: CELLULAR SENESCENCE / GOLD NANOPARTICLES / REACTIVE OXYGEN SPECIES

CHALERMSRI CHAYUTSATID: Evaluation of gold nanoparticles effect on cellular senescence change in preadipocyte (3T3-L1) and fibroblast (NIH 3T3) cell lines induced with hydrogen peroxide. ADVISOR: ASST. PROF.AMORNPUN SEREEMASPUN, M.D., Ph.D., CO-ADVISOR: DR.NARISORN KONGRUTTANACHOK, 63 pp.

Currently, gold nanoparticles (AuNPs) are popular to the implementation for many fields because of their exclusive features and high stability which are notably different from other nanoparticles. Indeed, skin care and anti-aging product use AuNPs for delivering active ingredients to the skin. Although many studies reported the benefits of AuNPs in terms of anti- senescent cells, there were some studies claimed that they also induced senescent cells. This study aimed to evaluate the effect of AuNPs on the cellular senescence change in preadipocyte and fibroblast cells. There were the uses of hydrogen peroxide for inducing senescent cells and the different size and concentration of AuNPs for this experiment. To test the effect of AuNPs to cytotoxicity on cells, aging phenotypes, free radical on cells, and cellular senescence mechanism. The results of this study were found that 50 ppm concentration of AuNPs size in 10 nm had cytotoxicity on both types of cells. AuNPs size in 10 nm and 20 nm were able to protect the occurrence of senescent cells phenotype notably on the preadipocyte cells only. On the contrary, AuNPs size in 10 nm and 20 nm were not able to stimulate the occurrence of free radical in both types of cells at all. From this, it was concluded that the cells response on aging was independent to free radical on cells. Furthermore, AuNPs size in 10 nm and 20 nm enabled to increase the SIRTUIN1 and p53 mRNA expressions, but decrease the C/EBPa and PPARg mRNA expressions on the preadipocyte cells only.

Field of Study: Medical Science
Academic Year: 2015

Student's Signature .....
Advisor's Signature .....
Co-Advisor's Signature .....

ACKNOWLEDGEMENTS

First of all, my deepest gratitude is to my advisor, Assistance Professor Amornpun Sereemaspun M.D., Ph.D., Anatomy Department, faculty of Medicine, Chulalongkorn University for giving me the opportunity, supervision, valuable coments and suggestions throughout my study

I am grateful to my thesis committee members, Professor Vilai Chentanez M.D., Ph.D., Associate Professor Padet Siriyasatien M.D., Ph.D., Dr. Narisorn Kongruttanachok, Dr. Dephicha Jindatip and for their guidance, generosity, and constructive comments in my thesis

I would like to thank my friends at Nanobiomedicine laboratory for their helpfulness, encouragement, and friendship which made me feel comfortable.

I would like to express my gratitude to all my teacher who put their faith in me and urged me to do better

Most importantly, I am grateful to my beloved family who gave a constant source of love, concern and support.

For the completion of my thesis, I appreciate the financial support from Ratchadapisek sompoj Fund, Faculty of Medicine, Chulalongkorn University (RA58/053).

CONTENTS

LIST OF FIGURES

LIST OF TABLES

CHAPTER I
INTRODUCTION

Nanomaterials are of interest in many biomedical because of their applications in large surface to volume ratio.[1] Certainly, many cosmetics and anti-aging products utilize nanoparticles that play a vital role in delivering active ingredients to the skin.[2]

Currently, gold nanoparticles (AuNPs) have been widely used for the treatment of diseases, diagnostic applications, drug delivery, gene therapy, imaging contrast agents[3], and especially ingredient of cosmeceuticals and anti-aging products.[4] They are well known in their chemical stability, biocompatibility, and simple synthesis.[5] However, while previous studies reported that AuNPs had toxicity on cells[6], many had described non-toxicity and reduction of free radical.[7, 8] It is still questionable whether the exogenous material nanogold can cause cellular aging as same as other xenogenic micro/nano particles.

Cellular senescence or cellular aging is a process which cells irreversibly arrest in proliferation and have specific changes in cell function, cell morphology and gene expression as well as epigenetic modifications.[9] These changes may contribute to age-associated diseases and affect to human life span. Biochemical markers are usually used for senescent cells such as senescence-associated beta-galactosidase (SA-β-gal), senescence-associated heterochromatin foci (SAHF) formation and overexpression of tumour suppressor gene (p53, $p21^{WAF-1}$ and $p16^{INK-4a}$).[10, 11]

Free radicals or reactive oxygen species (ROS) are one of the factors that are able to induce cellular senescence. The presence of ROS and loss of ROS scavenger on cells result in oxidative stress leading to cellular damage or cellular senescence.[12] In term of stress-induced premature senescence (SIPS), they have been used to induce premature senescence such as ultraviolet (UV) light, hyperoxia,

mitomycin C, tert-butylhydroperoxide (t-BHP) and hydrogen peroxide (H_2O_2). H_2O_2 is commonly used as SIPS during a short period of time.[13]

Recently, many researchers had extensively studied about biomolecules of cells related to cellular senescence. The most special interest was SIRTUIN1 (SIRT1), NAD^+-dependent deacetylase, is transcription factor and cofactor for target of histone and non-histone proteins.[14] SIRT1 has an influence on the function of cells against oxidative stress, glucose and lipid metabolism and DNA stability by deacetylating several substrates. Therefore, SIRT1 is used as one of biomarkers for human lifespan.[15]

The objective of this study aimed to evaluate the effect of gold nanoparticles on cellular senescence change in preadipocyte (3T3-L1) and fibroblast (NIH 3T3) cell lines. We assessed aging phenotype after cells were exposed to 10 and 20 nm AuNPs in concentration of 5 and 50 ppm on 3T3-L1 and NIH 3T3 cells. Furthermore, we investigated the alterations in mechanism of cellular senescence including p53, $p21^{WAF1}$ and $p16^{INK4a}$ expression. Finally, we observed mRNA expression level of adipogenesis transcriptional regulation (C/EBPα and PPARγ) in 3T3-L1 cells only.

Research questions of this study

1. Do the different sizes and concentrations of gold nanoparticles have cytotoxicity on 3T3-L1 and NIH 3T3 cells?

2. Are the gold nanoparticles able to affect cellular senescence change on 3T3-L1 and NIH 3T3 cells?

Objectives of this study

1. To study cytotoxicity of gold nanoparticles on 3T3-L1 and NIH 3T3 cells.

2. To evaluated the effect of gold nanoparticles about cellular senescence change on 3T3-L1 and NIH 3T3 cells.

Hypothesis of this study

1. Gold nanoparticles at small size and high concentration have cytotoxicity on 3T3-L1 and NIH 3T3 cells.

2. Gold nanoparticles are able to affect cellular senescence change on 3T3-L1 and NIH 3T3 cells.

Expected outcome of this study

1. To apply the knowledge from this study to choose appropriate physical of gold nanoparticles to use for anti-aging products.

2. To obtain the basic knowledge of effect of gold nanoparticles about cellular senescence change on 3T3-L1 and NIH 3T3 cells.

3. To obtain the basic for understanding the aging phenotypes and mechanisms modulating of cellular senescence by gold nanoparticles.

Conceptual framework

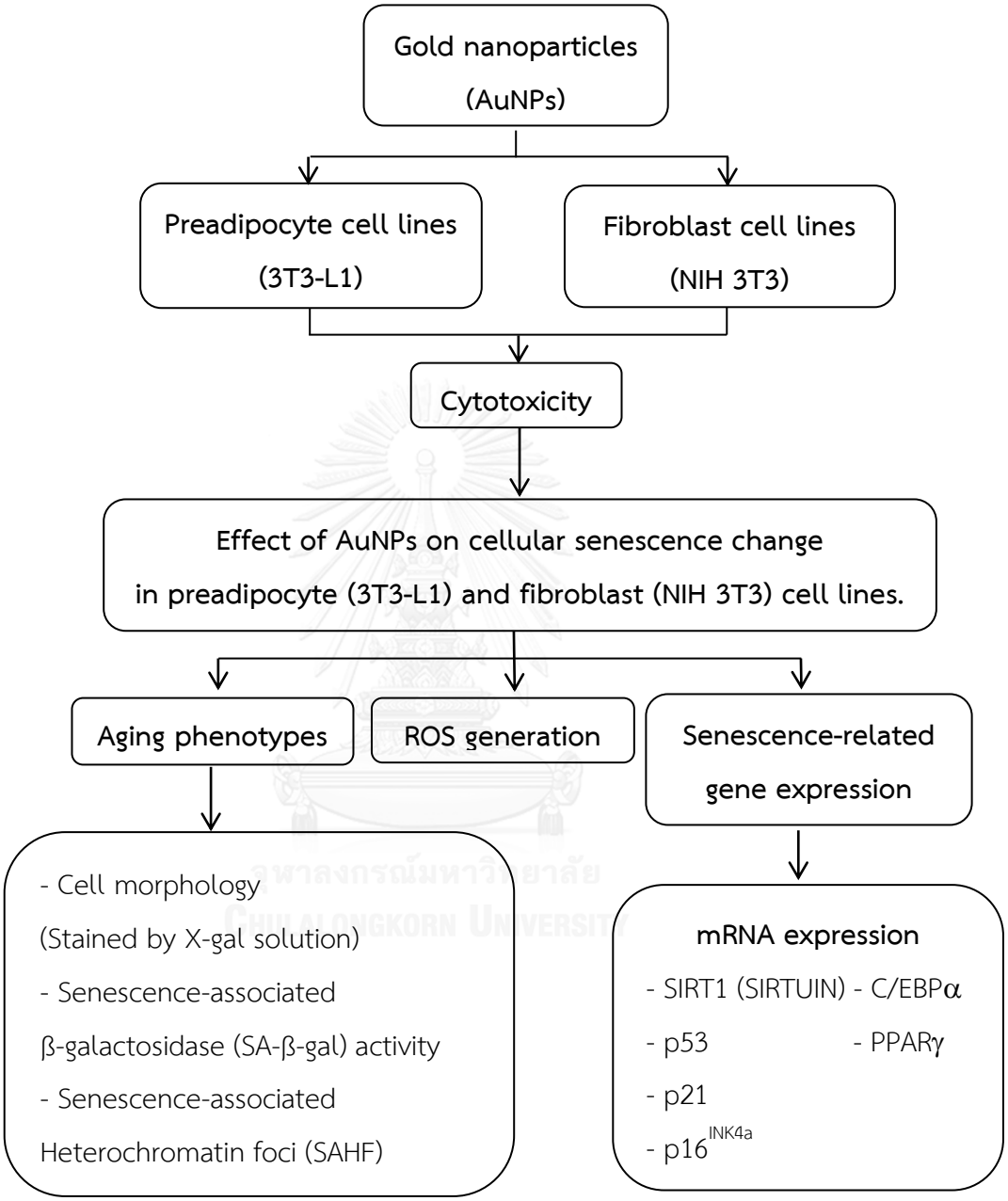

CHAPTER II
LITERATURE REVIEW

Nanotechnology

Nanotechnology has been interested for many decades. It is about manipulating atoms and molecules to create systems, devices, and materials which are size range in 1 to 100 nanometers and its dimension has at least one dimension enable to be nanomaterial. Nanomaterial can be applied in many fields such as physics, engineering, chemistry, and medicine. In the medicine, they have extensively used nanomaterial such as drug delivery, gene therapy, medical imaging and diagnostics due to their special properties of nanomaterial including large surface to volume ratio and physical and chemical properties that can be adjust size and shape.[1] Over the past several years, scientists have been tried to develop nanomaterial and construct many nano structures especially nanoparticles.[16] Nanoparticles have been widely used in many commercially available products such as medicines, pharmaceuticals, cosmesuticals, sport equipment, sunscreens, soaps, moisturizers, shampoos, and detergents etc.[17]

Gold nanoparticles (AuNPs), one of nanomaterials, are widely investigated due to their unique properties are different than other nanoparticles including, biocompatibility, chemical stability, unique optical properties, and simple synthesis.[5] Presently, AuNPs are used in a wide range for biological applications and crucial ingredient of cosmetics and beauty care products.[4] There are many advertorial refer to advantage of AuNPs in many anti-aging products.[18-21] For example,

- Penetration deep into the skin and promoting collagen synthesis
- Reducing aging process and maintaining skin youthful appearance
- Accelerating blood circulation
- The transport of active ingredient into cell
- Reducing fine lines and wrinkles of skin
- Promoting the firmness and elasticity of skin
- Defense against free radicals
- Antiseptic and anti-inflammatory properties
- Anti advanced glycation end products (AGEs)

However, previous study reported that AuNPs was able to exert cytotoxicity reactive oxygen species (ROS) and accelerate cellular senescence. The following context briefly shows the cytotoxicity and cellular aging by AuNPs from previous studies.

In 2006, Pernodet N *et al*. revealed citrate/gold nanoparticles size in 14 nm at concentration of 0.1 and 0.6 mg/ml crossed cell membrane and accumulated into vacuoles after treatment for 6 days in human dermal fibroblasts. There were loss of actin filaments and extracellular matrix constructs. Moreover, cell proliferation, adhesion, and motility were decreased after exposure to citrate/gold nanoparticles. The researchers suggested possible mechanisms of specific genes expressed and proteins produced.[22]

In 2008, Li JJ *et al*. studied oxidative damage of gold nanoparticles in lung fibroblasts. They found that 20 nm AuNPs at a concentration of 1.0 nM decreased cell proliferation after exposure to AuNPs for 72 h by downregulation of specific cell cycle genes such as MAD2, Cyclin B2 and Cyclin B1 and reduction the expression of critical checkpoint proteins and also found autophagy. They supposed that it have been caused a cellular against oxidative stress.[23]

In 2009, Qu Y and Lu X studied the effect of gold nanoparticles on human dermal fibroblasts fetal (HDF-f). The cytotoxicity was evaluated by MTT assay. The results showed that approximately 20 nm GNPs did not cause cell death at a concentration of 300 mM. Higher concentrations of AuNPs affected on cell morphology of HDF-f.[24]

In 2010, Lu S *et al*. investigated the effect of AuNPs size in 34 nm at different concentration on proliferation of primary keratinocyte cell. The results showed 5 ppm 34 nm AuNPs stimulated keratinocyte proliferation and promoted cell growth, but more than 10 ppm 34 nm AuNPs had a toxicity to keratinocytes. These data suggested that low concentration of AuNPs might have been used in biomedical application.[25]

In 2010, Mironava T *et al*. investigated the effect of AuNPs on human dermal fibroblasts. The results showed that AuNPs penetrated plasma membrane and accumulated in large vacuoles and did not penetrate either nucleus or mitochondria. Cell doubling time was increased after 13 and 45 nm AuNP exposure with higher concentration and longer exposure. Besides, they demonstrated the recovery of cells after AuNP removal. The results showed that AuNPs did not change in actin or beta-tubulin protein levels. However, extracellular matrix (ECM) proteins,collagen and fibronectin, were decreased after AuNP removal. These data indicated that cells recovered a function depending on size, concentration and exposure time.[26]

In 2013, Coradeghini R *et al*. studied the effects of AuNPs on Balb/3T3 mouse fibroblasts. The results showed that cell viability was decreased after treatment with AuNPs size in 5 nm at concentration more than 50 μM for 72 h. They observed AuNPs size in 15 nm at all concentrations and exposure times had not toxicity on fibroblast cells.[27]

In 2014, Mironava T *et al*. discovered AuNPs size in 13 and 45 nm at concentration of 142 and 13 mg/ml, respectively penetrated in human adipose-derived stromal cells (ADSCs) and stored in vacuoles. Population doubling times were increased after exposure to AuNPs. They found a decreasing of cell motility and cell-mediated collagen contraction. Moreover, smaller particles and higher concentration had the same effect as the larger size. Importantly, AuNPs reduced adipogenesis as measured by lipid droplet accumulation and adiponectin secretion. They demonstrated the recovery of cells after AuNP removal. The level of AuNPs in ADSCs decreased and ADSCs functions were restored. The researchers suggested about careful of size, concentration and using for medical application.[28]

Cellular senescence

Cellular senescence is a process of cells which they will be chosen instead of either cancer or apoptosis pathway that it has associated with aged-related diseases and human life span. In 1961, Hayflick and Moorhead defined the senescent cells, which are an irreversible growth arrest. They found human fibroblast was limited cell proliferation after cells entered into growth arrest and stopped cell proliferation even though cells had sufficiently the area and nutrients for growth. The morphology of senescent cells had a larger cell shape, flattened cells, enlarged nucleoli, and containing many vacuoles.[29, 30]

Reactive oxygen species (ROS) are one type of free radical. Previous reports showed that reactive oxygen species induced the tumor suppressor p53 protein and pRB, leading to premature senescence.[31, 32] ROS are produced by endogenous source such as mitochondria during cellular respiration and inflammation. Other environmental pollution and ultraviolet (UV) light exposure are exogenous source. It is an unstable molecule and susceptibility of responding with DNA, RNA and other molecules.[33]

In the past, cellular senescence was associated with telomere shortening which it occurs at the end of chromosomes. Normal DNA replication for cell division, chromatin will lose a telomere and become a very short until it is unable to divide. Previous study reported that using the telomere was not suitable for senescence biomarker because there are problems in interpretation and least accuracy.[34]

The current interest in attention is the study about other biomolecules of cells entirely related to senescense, and the ones were in special interest such as senescence-associated ß-galactosidase (SA-ß-gal), senescence-associated heterochromatin foci (SAHF), and SIRTUIN1. The increasing of SA-ß-gal or lysosomal ß-D-galactosidase enzymes is one of the most commonly used senescence biomarker. Its increased ß-D-galactosidase activity by which overexpression

of GLB1 is encoded. In quiescence cells, they show ß-D-galactosidase activity in lysosomals that functions optimally at pH 4, and senescent cells show ß-D-galactosidase activity in the lysosomals that functions optimally at pH 6.[35] These different functions of enzymes are able to identify cellular senescence. Additionally, it is well known, cellular senescence is associated with altered chromatin structure in nuclei. Senescent cells display package and condense chromatin, it is called a senescence-associated heterochromatin foci (SAHF). The past decade had extensively studied about biomolecules of cells related to senescense.[11] The most special interest was expression of SIRTUIN1 or SIRT1. SIRT1 plays a role in protection of cells against oxidative stress, regulating glucose homeostasis, lipid metabolism, and p53 deacetylation resulting in decreasing apoptosis and reducing aging process.[36]

Recently, there have been many researches about fibroblast aging. However, there are few studies investigating the preadipocyte aging. Preadipocytes are commonly found in hypodermis layer of skin. The main role of preadipocytes is to generate new fat cells which help in storing energy, thermoregulation, mechanical protection, immune and endocrine function, and process of hair growth.[37] Previous reports have been discovered that CCAAT / enhancer binding protein-alpha (C/EBPα) and peroxisome proliferator-activated receptor-gamma (PPARγ) had lower in preadipocyte aging result in decrease preadipocyte replication and increasing lipotoxicity and chemokine. C/EBPα and PPARγ are adipogenesis transcriptional regulator involved in regulating downstream adipogenic genes, sustained activity of insulin-responsive fat cells and down-regulating the pro-inflammatory.[37] The following context briefly shows the previous research of biomolecules related to cellular senescence.

In 2000, Toussaint O *et al*. reported that human dermal fibroblasts (HDFs) after exposure to H_2O_2 were exhibited a senescent phenotype and overexpression of collagenase, matrix-metalloproteinase-1, IFN-γ and MnSOD. H_2O_2-exposed cells were blocked mainly in the G1 phase of the cell cycle, by p53 and cyclin-dependent kinase Inhibitors; including $p21^{WAF1}$ and $p16^{INK4a}$ which were overexpressed.(38)

In 2002, Langley E *et al*. investigated the function of SIRT1 protein (human homolog of yeast Sir2 protein). They found that SIRT1 deacetylated p53 and repressed PML/p53-induced cellular senescence. They proposed that SIRT1 deacetylase enzyme was a novel regulator of p53 function for modulating cellular senescence.(39)

In 2004, Munro J *et al*. revealed that histone deacetylase inhibitors (HDACIs) sodium, dibutyrate (SDB) and trichostatin A (TSA) induced a replicative senescence in human fibroblasts. They found that cell cycle inhibitors $p21^{WAF1}$ and $p16^{INK4A}$ were upregulated by SDB-treated cells and $p16^{INK4A}$/pRb pathway was the major mediator of HDACIs-induced senescence in cells. Moreover, p53 pathway was the major pathway for senescence in mouse fibroblasts.(40)

In 2010, Mirzayans R *et al*. studied the relationship between p16/p21 levels and senescence by exposure to ionizing radiation in various human fibroblast strains. (normal, ataxia telangiectasia (AT) and Li-Fraumeni syndrome (LFS). At late passages, all strains had flattened and enlarged cell morphology, and senescence-associated ß-galactosidase positive. p21 pathway was the major mediator of ionizing radiation-induced senescence in p53-proficient (normal and AT) fibroblasts. In p53-deficient (LFS) fibroblasts, p16 pathway was the major mediator of ionizing radiation-induced senescence.(41)

In 2013, Monickaraj F *et al*. investigated oxidative stress generation, shortened telomeres, senescence and functional impairment in adipocytes (3T3-L1). They used various oxidative stressors for inducing cellular senescence such as H_2O_2, glucose oxidase, asymmetric dimethylarginine (ADMA), and glucose oscillations. The results showed both ROS generation and DNA damage was increased in cells after exposure to oxidative stress. Besides, oxidative stress-exposed 3T3-L1 cells showed shortened telomeres and increased mRNA and protein expression of p53, p21, TNFα and IL-6. Moreover, adiponectin levels were decreased in cells after exposure to oxidative stress with impaired glucose uptake. Furthermore, ROS generation, DNA damage, shortened telomeres and pro-inflammatory phenotype were increased in cells after exposure to oxidative stress with impaired glucose uptake.[42]

In 2015, Kilic U *et al*. studied the association between genetic variation in SIRT1 and phenotype at different ages and observed relation with levels of SIRT1, eNOS, PON-1, cholesterol, TAS, TOS, and OSI in human population. They discovered an increasing SIRT1 level in older people and a positive correlation between SIRT1 level and age in the overall studied population. Older people had lower PON-1 levels than adults and children which may have explained the high levels of SIRT1 protein as a compensatory mechanism for oxidative stress in the elderly. The eNOS protein level was decreased in older people when compared to adults. OSI TAS and TOS levels were increased in older people suggesting an increase in oxidative stress.[43]

CHAPTER III
MATERIALS AND METHODS

Cell culture

Preadipocyte (3T3-L1) and fibroblast (NIH 3T3) cell lines were cultured in Dulbecco's Modified Eagle Medium (DMEM) (Gibco, USA) containing 10%(v/v) fetal bovine serum (FBS) (Gibco, USA) and 1% (v/v) antibiotic antimycotic (Gibco, USA) at 37°C in 5% CO_2. Cells at early passages (below 30 passages) were used in cell experiments to avoid complications of replicative senescence. After 3T3-L1 and 3T3 cell lines reached 90% confluence, cells were sub-cultured the use of 0.25% trypsin/EDTA (Gibco, USA)

Gold nanoparticles (AuNPs) synthesis and characterization

AuNPs size in 10 nm was purchased from sigma andrich (lot MKBW1502V), and AuNPs size in 20 nm was synthesized in laboratory. Briefly, 1 mL of 1% hydrogen tetracholoaurate (III) trihydrate ($HAuCl_4.3H_2O$) was added into 34 mL milliQ water and stirring vigorously. 12 mL of 0.0202 M trisodium citrate dihydrate ($Na_3C_6H_5O_7.2H_2O$) was added into 3 mL milliQ water and stirring vigorously. 15 mL of trisodium citrate dehydrate solution was transferred to hydrogen tetracholoaurate (III) trihydrate solotion. The solution in the flask would change the colour from yellow to lightly red. The lightly red colour could indicate the formation of AuNPs. AuNPs was measured with the particle surface charged by Zetasizer nano series (Malvern Instruments, England) and observed nanoparticle morphology at 100 kV by transmission electron microscopy (TEM) (Hitachi, Japan).

Induction of premature senescence cells with H_2O_2

To induce premature senescence, 3T3-L1 and NIH 3T3 cells were exposed to H_2O_2 at 100 μM for 2 h in medium. After this exposure, the cells were washed with phosphate buffer solution (PBS) to remove H_2O_2 and re-culture in fresh complete medium for 72 h. The control cultures were followed by the same schedule of medium changes without H_2O_2 treatment.

AuNP treatment

3T3-L1 and NIH 3T3 cells at half-confluence were exposed to AuNPs sizes in 10 and 20 nm AuNPs at concentrations of 5 and 50 ppm for 24 h. Cells were washed by PBS and fresh completely medium replaced. To observe the effect of AuNPs on the premature senescence of 3T3-L1 and NIH 3T3 cells due to H_2O_2, the cells were pre-treated by AuNPs sizes in 10 and 20 nm at concentrations of 5 and 50 ppm for 24 h after inducing with 100 μM H_2O_2 for 2 h then re-culture in fresh complete medium for 72 h.

Cytotoxicity test

The cellular cytotoxicity was confirmed by cell viability using PrestoBlue™ reagent (Invitrogen, USA). 3T3-L1 and NIH 3T3 cell lines were seeded into 96-well plates at density of $5x10^3$ cells/well in 100 μL of complete medium and incubated at 37°C under 5% CO_2 atmosphere for 12 h. Cells were washed by PBS twice and treated with various concentrations of AuNPs size in 10 and 20 nm (5 and 50 ppm) in 90 μL for 24 and 72 h. Cells were added 10 μL of PrestoBlue™ reagent and incubated for 30 min. Fluorescence was measured using a microplate reader at 560 and 590 nm (Thermo, Varioskan flash, England). It was found that the percentage of cell viability was calculated by normalize to control group.

Senescence-association beta-galactocidase (SA-ß-gal) staining

To identify premature senescence, we previously needed to describe briefly about the cells.[44] They would be washed by PBS and fixed in 3.7% (v/v) formaldehyde for 5 min at room temperature. After that the cells were incubated in an SA-ß-gal staining solution (1 mg/mL 5-bromo-4-chloro-3-indolyl ß-D-galactosidase (x-gal), 40 mM citric acid (pH 6.0), 40 mM sodium phosphate (pH 6.0), 5 mM potassium ferrocyanide, 5mM potassium ferricyanide, 150 mM sodium chloride and 2 mM magnesiumchloride) overnight at 37°C. The senescent cells were also stained in blue when it viewed under a Nikon Eclipse Ti inverted microscope (Nikon, Japan).

Senescence-association beta-galactocidase (SA-ß-gal) activity

The SA-ß-gal activity was confirmed by ONPG enzyme assay. Briefly, equal numbers $1x10^5$ of cells were harvested in a microcentrifuge tube after washing once with PBS. The cells were lysed with 33.3 mL of a 0.1M sodium citrate buffer (pH 6.0) followed by four cycles of freezing with liquid nitrogen and thawing in a 37°C water bathing. The lysate was centrifuged at 12,000xg for 7min. The supernatant was transferred to a new centrifuge tube and added 33 mL of ONPG (4 mg/mL), 3mL of 0.5M MgCl2, 84mL of 0.1M sodium citrate buffer (pH 6.0). The tube was vortexed to mix the solution and incubated at 378C for 12 h. This reaction was developed and quenched by the addition of two volumes of 1M Na_2CO_3, and 200 mL was also transferred to 96-well plate. Fluorescence was measured using a microplate reader at 420 nm (Thermo, Varioskan flash, England).

Senescence-association heterochromatin foci (SAHF)

To determine SAHF, cells were washed with PBS and fixed with cold absolute methanol for 5 min at room temperature. Cells were incubated in freshly prepared 0.3 µM DAPI for 30 min. The SAHF were visualized by using a Nikon Eclipse Ti-E confocal laser scanning microscope (Nikon, Japan)

Reactive oxygen species (ROS) generation

Intracellular reactive oxygen species (ROS) production was confirmed by 2',7'– dichlofluoreceine-diacetate (H_2DCF-DA) assay (Molecular probes™, USA). Briefly, 3T3-L1 and NIH 3T3 cell lines were seeded into 96-black well plates at density of $1x10^4$ cells/well in 100 µL of complete medium and incubated at 37°C under 5% CO_2 atmosphere for 12 h. Cells were washed by PBS twice. After, cells were added 100 µL of working H_2DCFDA and Incubated for 30 min at 37°C in dark place. Cells were washed by PBS twice and treated various concentrations of AuNPs size in 10 and 20 nm (5 and 50 ppm) in 100 µL for 1 and 24 h. Fluorescence was measured using a microplate reader at 485 nm and 528 nm (Thermo, Varioskan flash, England). It was found that the percentage of ROS generation was calculated by normalize to control group.

RNA extraction and quantitative real-time PCR

3T3-L1 and NIH 3T3 cell lines were seeded into 24-well plates at density of $1x10^5$ cells/well in 500 µL of complete medium and incubated at 37°C under 5% CO_2 atmosphere for 12 h. Cells were washed by PBS twice and exposed to AuNPs at various concentrations of 10-nm AuNPs (5 and 50 ppm) and 20-nm AuNPs (5 and 50 ppm) for 24 h. Cells were washed by PBS and completely medium replaced. To observe the effect of AuNPs on the premature senescence of 3T3-L1 and 3T3 cell lines due to H_2O_2, the cells were pre-exposed to AuNPs for 24 h followed by 100 µM H_2O_2 treatment for 2 h and fresh complete medium for 72 h. The total RNA was isolated from cells by using TRIzol reagent (Invitrogen). One microgram of total RNA was used for cDNA synthesis with the First strand cDNA synthesis kit (Roche®) regarding the manufacturer's instructions. Real-time PCR system used the Express SYBR GreenER qPCR Supermix Universal (Invitrogen). The cDNA was also used as a template for measurement SIRT1, p53, p21, p16

, C/EBPα and PPARγ gene expression. Primer sequences were already listed in Table 1. Quantitative Real-time PCR performed the use of StepOnePlus Real-Time PCR System (ABI Applied Biosystems). The C_T (threshold cycle) values obtained the target genes which were normalized to the endogenous B-actin level (housekeeping gene), and related to the normalized calibrator.

ΔCt (sample) = Ct (target gene of sample) - Ct (reference gene of sample)

ΔCt (calibrator) = Ct (target gene of calibrator) - Ct (reference gene of calibrator)

Ct was the point at the fluorescence crossed the threshold. Then, Δ ΔCt and Ratio (folds of difference) of sample: calibrator was calculated by using the following equation.

$$\Delta\Delta Ct = \Delta Ct \text{ (sample)} - \Delta Ct \text{ (calibrator)}$$

$$\text{Ratio (folds of difference) of sample: calibrator} = 2^{-\Delta\Delta Ct}$$

Table 1. Sequence of primers used in RT-qPCR

Genes	Primers	Sequences 5'-3'	Annealing Temp.	References
p53	Forward Reverse	TTC-TGT-AGC-TTC-AGT-TCA-TTG-G ATG-GCA-GTC-ATC-CAG-TCT-TC	57 °C	Finny Monickaraj, *et al.* (2013)[42]
p21	Forward Reverse	TGC-ATC-CGT-TTC-ACC-CAA-CC CTC-ATT-TTT-CCA-AAG-TGC-TAT-TCA-GG	57 °C	Finny Monickaraj, *et al.* (2013)[42]
$p16^{INK4a}$	Forward Reverse	CCC-AAC-GCC-CCG-AAC-T GTG-AAC-GTT-GCC-CAT-CAT-CA	57 °C	Jin Zhang, *et al.* (2014)[45]
SIRT1	Forward Reverse	CAC-AAA-TAC-TGC-CAA-GAT-GTG-AAT- TCC-AAA-ATA-TTA-CAC-TCT-CCC-CAG-TA	57 °C	Maya E. Kotas, *et al.* (2013)[46]
C/EBPα	Forward Reverse	CGC-AAG-AGC-CGA-GAT-AAA-GC CAC-GGC-TCA-GCT-GTT-CCA	60 °C	Cheng Huang, *et al.* (2006)[47]
PPARγ	Forward Reverse	CGC-TGA-TGC-ACT-GCC-TAT-GA AGA-GGT-CCA-CAG-AGC-TGA-TTC-C	60 °C	Cheng Huang, *et al.* (2006)[47]
B-actin	Forward Reverse	ACC-TTC-TAC-AAT-GAG-CTG-CG CTG-GAT-GGC-TAC-GTA-CAT-GG	57 °C	Jennifer A. Rose, (2011)[48]

PCR conditions for each primer couple were shown as follow: pre-PCR heat step 50°C for 2 min, 95°C for 2 min was required to activate the enzyme in real-time kits, pre-denaturation step at 95℃ 10 min, followed by 40 cycles of denaturation at 95℃ 15 sec, annealing temperature shown in Table 1 at 1 min and extension at 72℃ 3 min.

Statistical analysis

All analyses were performed using GraphPad Prism 5. One-way ANOVA (analysis of variance) followed by the Tukey's multiple comparison tests used for comparative between groups. A p value < 0.05 was considered statistically significant.

CHAPTER IV
RESULTS AND DISCUSSION

RESULTS

Characterization of gold nanoparticles (AuNPs)

Gold nanoparticle sizes were measured by transmission electron microscope (TEM). The sample of AuNP solution were prepared by dropped on the carbon coated copper grids and then allow it to evaporate under vacuum. The result showed that AuNPs have spherical morphology and average sizes approximately 10 and 20 nm (figure 1A, 1B). Furthermore, stability and surface charge of nanoparticles are represented strongly cationic or anionic. Zeta potential should be greater than +30 mV or less than -30 mV. The zeta-potential result showed a positive/negative charge both size of AuNPs (Table 2).

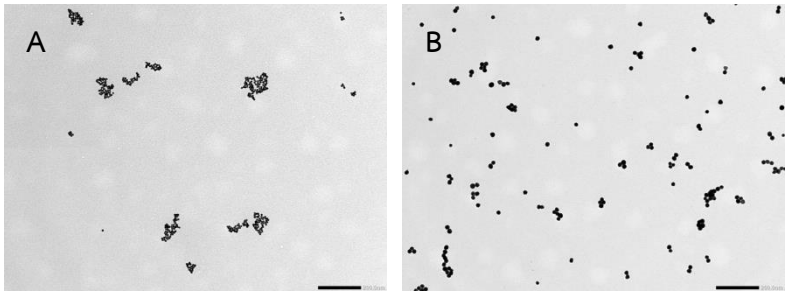

Figure 1. Characterization of citrate-stabilized AuNP synthesis. TEM image of monodisperse citrate-stabilized 10 nm AuNPs (A). TEM image of monodisperse citrate-stabilized 20 nm AuNPs (B). The sample was prepared by drying placed of the aqueous solution of nanoparticles on the coated copper grids.

Table 2. Zeta potential measurements to characterize the surface AuNPs in different size.

Size of AuNPs (nm)	Zeta Potential (mV)
10	-37.30
20	30.64

Cell viability

To show the effect of AuNPs on cell viability of 3T3-L1 and NIH 3T3 cell lines, cell viability was measured by Prestoblue™ assay. Percentage of cell viability of 3T3-L1 and NIH 3T3 cells treated by AuNPs are shown in Figure 2. Cells were treated by 10 and 20 nm AuNPs at concentrations of 5 and 50 ppm for 24 and 72 h. DMEM was used as a control.

In 3T3-L1 cells, cell viability was significantly increased after treatment of cells by 5 ppm 10 nm AuNPs and 5 and 50 ppm 20 nm AuNPs for 24 and 72 h when it was compared to control group (Figure 2A, 2B). However, cell viability was significantly decreased after treatment of cells by 50 ppm 10 nm AuNPs for 24 and 72 h when it was compared to control group (Figure 2A, 2B).

In NIH 3T3 cells, cell viability was significantly increased after treatment of cells by 5 ppm 10 nm AuNPs and 5 and 50 ppm 20 nm AuNPs for 24 and 72 h when it was compared to control group (Figure 2C, 2D). Cell viability was not significantly different after treatment of cells by 50 ppm 10 nm AuNPs for 24 h (Figure 2C), but significantly decreased after treatment of cells by 50 ppm 10 nm AuNPs when it was compared to control group at 72 h (Figure 2D).

Preadipocyte (3T3-L1)

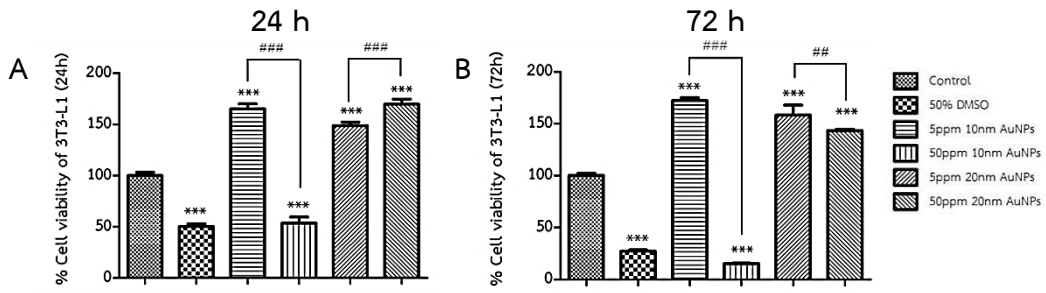

Fibroblast (NIH 3T3)

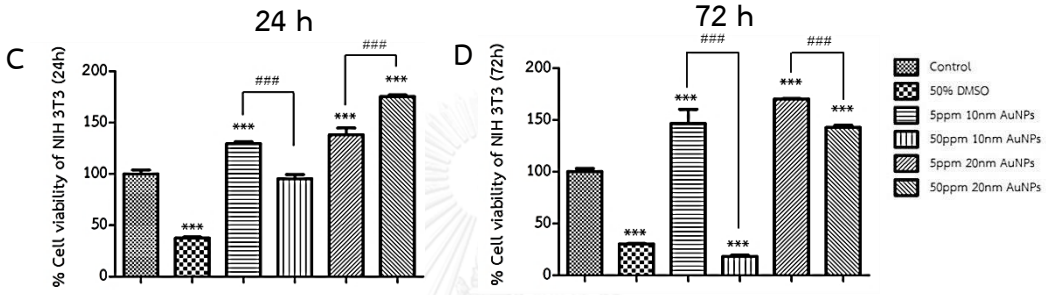

Figure 2. Cell viability of 3T3-L1 and NIH 3T3 cells after exposure to AuNPs for 24 and 72 h. Percentage of cell viability in 3T3-L1 (A) and NIH 3T3 (C) cells after exposure to AuNPs at 24 h. Percentage of cell viability in 3T3-L1 (B) and NIH 3T3 (D) cells after exposure to AuNPs at 72 h.* indicates that differences are significantly compared with control group, # indicates that differences are significantly between the groups. Values are mean ± SD (n=3) significance indicated by: *, $^{\#}$ $p<0.05$, **, $^{\#\#}$ $p<0.01$ and ***, $^{\#\#\#}$ $p<0.001$

Aging phenotypes

Cell morphology

To show the effect of AuNPs on cellular morphological aging of 3T3-L1 and NIH 3T3 cell lines. Cells were stained with SA-β-gal solution. Senescent cells were stained in blue when it was viewed under an inverted phase contrast microscopy. Cells were treated and pre-treated by AuNPs size in 10 and 20 nm at concentrations of 5 and 50 ppm for 24 h. 100 μM H_2O_2 was used as a positive control.

In 3T3-L1 cells, treatment of cells by 10 and 20 nm AuNPs in both of concentration of treated AuNPs for 24 h, cells were unchangeable to cellular morphological aging when it compared to control group (Figure 3C-3F). Pretreatment of cells by 10 and 20 nm AuNPs in both of concentration of treated AuNPs for 24 h, cells were also unchangeable to cellular morphology when it compared to 100 μM H_2O_2 group (Figure 3G-3J). The number of cells was decreased after treatment of cells by 50 ppm 10 nm AuNPs for 24 h (Figure 3D). SA-β-gal-positive cells were not found all AuNP-treated and pretreated groups.

In NIH 3T3 cells, cells were unchangeable to cellular morphological after treatment of cells by 5 ppm 10 nm AuNPs for 24 h when it compared to control group (Figure 4C). However, treatment of cells by 50 ppm 10 nm AuNPs and 5 ppm and 50 ppm 20 nm AuNPs, cells showed extended, flattened, and enlarged nuclei when it compared to control group (Figure 4D-4F). Pretreatment of cells by 10 and 20 nm AuNPs in both of concentration of treated AuNPs for 24 h, cells showed extended, flattened, and enlarged nuclei when it compared to 100 μM H_2O_2 group (Figure 4G-4J). The number of cells was decreased after treatment of cells by 50 ppm 10 nm AuNPs for 24 h (Figure 4D). SA-β-gal-positive cells were found all AuNP-pretreated groups. The summary of cell morphology would be showed in table 3 and 4.

Preadipocyte (3T3-L1)

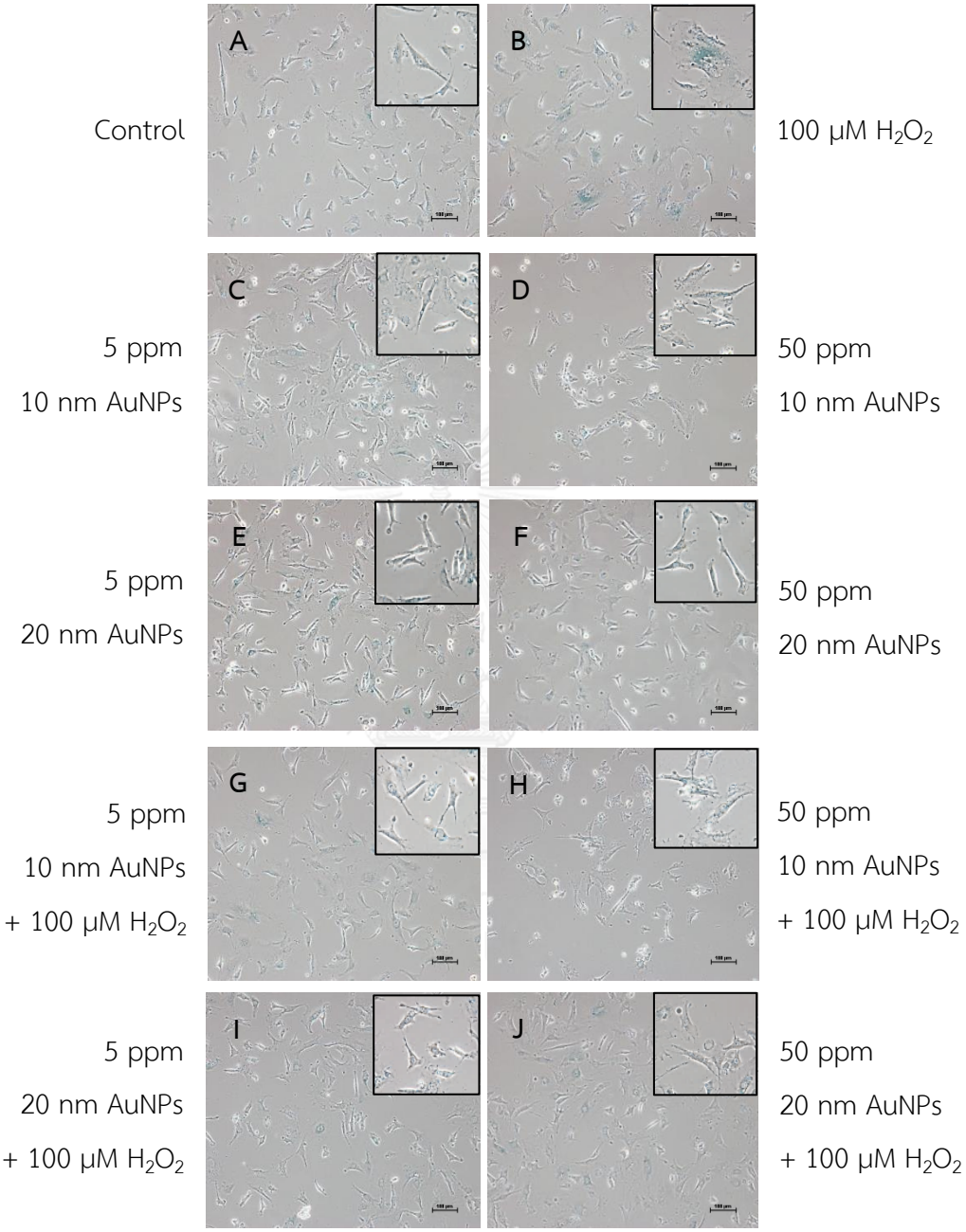

Figure 3. Cell morphology of 3T3-L1 cells after treatment and pretreatment by AuNPs size in 10 and 20 nmat concentrations of 5 and 50 ppm, 100x magnifications used.

Fibroblast (NIH 3T3)

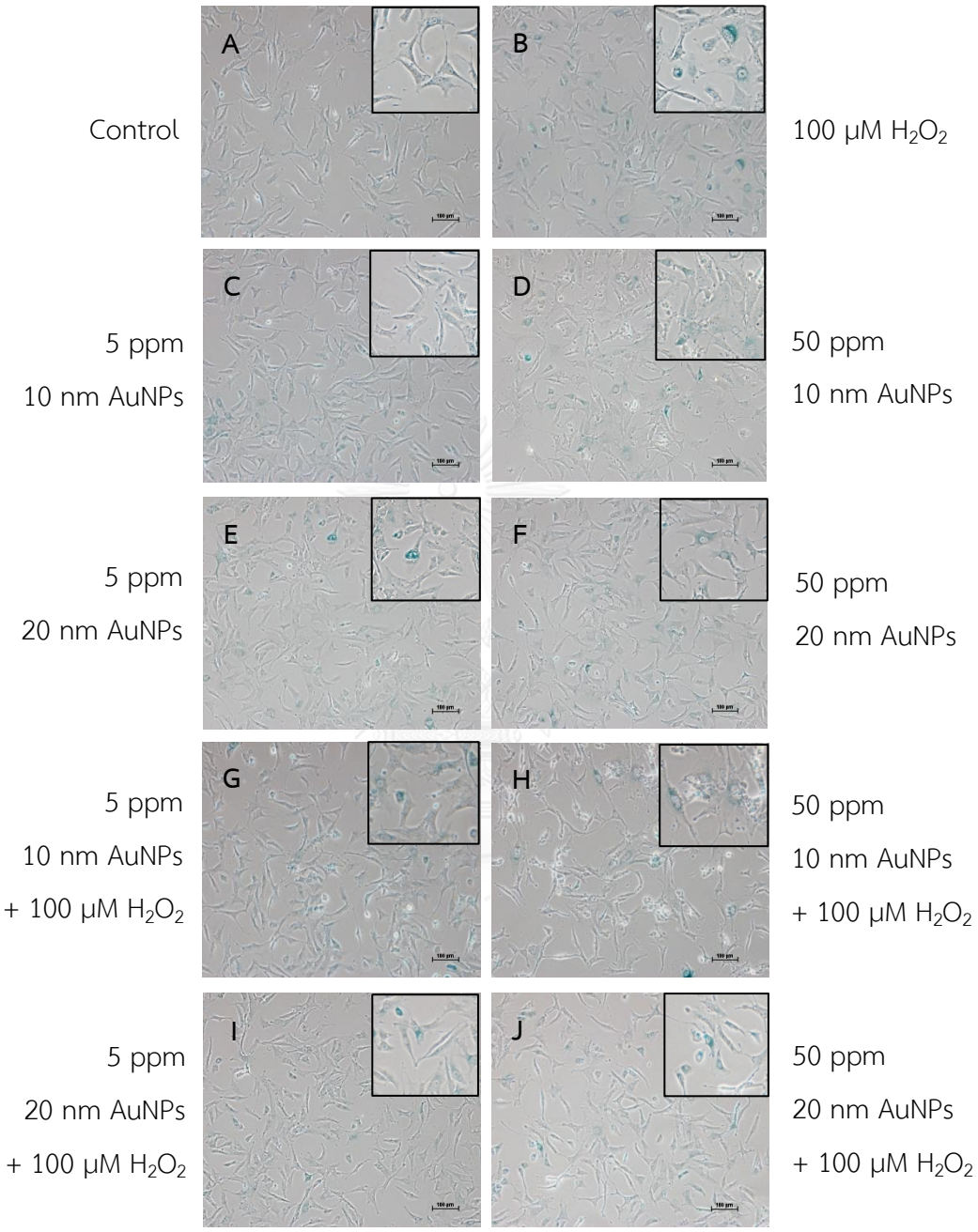

Figure 4. Cell morphology of NIH 3T3 cells after treatment and pretreatment by 10 and 20 nm AuNPs at concentrations of 5 and 50 ppm, 100x magnifications used.

Senescence-association beta-galactocidase (SA-ß-gal) activity

To show the effect of AuNPs on SA-ß-gal activity of 3T3-L1 and NIH 3T3 cell lines. Percentage of SA-ß-gal activity of 3T3-L1 and NIH 3T3 cells after treatment and pretreatment by AuNPs are shown in Figure 6. Cells were treated and pre-treated by AuNPs size in 10 and 20 nm at concentrations of 5 and 50 ppm for 24 h. 100 μM H_2O_2 was used as a positive control.

In 3T3-L1 cells, cells were significantly decreased for SA-ß-gal activity after treatment of cells by 10 and 20 nm AuNPs in both of concentration of treated AuNPs for 24 h when it was compared to control group. Compared to 100 μM H_2O_2 group, cells were significantly decreased for SA-ß-gal activity after pretreatment of cells by 10 and 20 nm AuNPs in both of concentration of treated AuNPs for 24 h (Figure 5A).

In NIH 3T3 cells, SA-ß-gal activity was not significantly different after treatment of cells by 5 ppm 10 nm AuNPs for 24 h when it compared with control group. Cells were significantly increased for SA-ß-gal activity after treatment of cells by 50 ppm 10 AuNPs and 5 and 50 ppm 20 nm AuNPs for 24 h when it compared to control group. In contrast, pretreatment of cells by 10 and 20 nm AuNPs in both of concentration of treated AuNPs for 24 h, cells were not significantly different in SA-ß-gal activity when it compared with 100 μM H_2O_2 group (Figure 5B). The summary of SA-ß-gal activity would be showed in table 3 and 4.

Preadipocyte (3T3-L1)

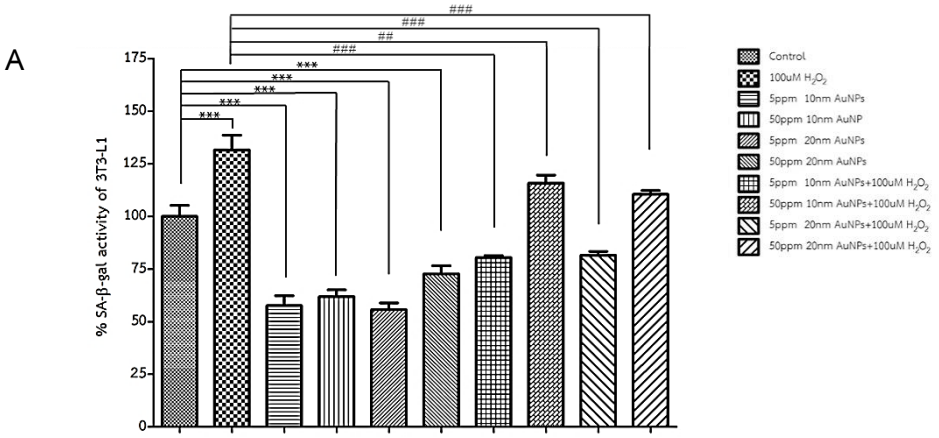

Fibroblast (NIH 3T3)

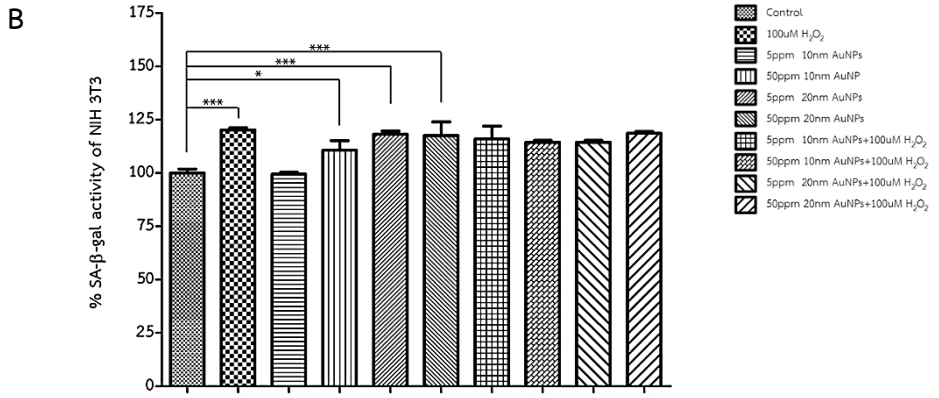

Figure 5. Senescence-association beta-galactocidase activity of 3T3-L1 and NIH 3T3 cells after treatment and pretreatment by 10 and 20 nm AuNPs at concentrations of 5 and 50 ppm. Percentage of SA-β-gal activity in 3T3-L1 after treatment and pretreatment by 10 and 20 nm AuNPs at concentrations of 5 and 50 ppm for 24 h (A). Percentage of SA-β-gal activity in NIH 3T3 after treatment and pretreatment by 10 and 20 nm AuNPs at concentrations of 5 and 50 ppm for 24 h (B). * indicates that differences are significantly compared with control group, # indicates that differences are significantly with 100 μM H_2O_2 group. Values are mean ± SD (n=3) significance indicated by: *, # p<0.05, **, ## p<0.01 and ***, ### p<0.001

Senescence-association heterochromatin foci (SAHF)

To show the effect of AuNPs on SAHF of 3T3-L1 and NIH 3T3 cell lines, cells were stained with 300 nM DAPI and showed punctate heterochromatin foci in nuclei, demonstrating SAHF-positive cells. Cells were treated and pre-treated by AuNPs size in 10 and 20 nm at concentrations of 5 and 50 ppm for 24 h. 100 μM H_2O_2 was used as a positive control. In 3T3-L1 and NIH 3T3 cells, treatment and pretreatment of cells by 10 and 20 nm AuNPs in both of concentration of treated AuNPs for 24 h showed no change of heterochromatin when it was compared to control and 100 μM H_2O_2 group (Figure 6, 7). The summary of SAHF would be showed in table 3 and 4.

Preadipocyte (3T3-L1)

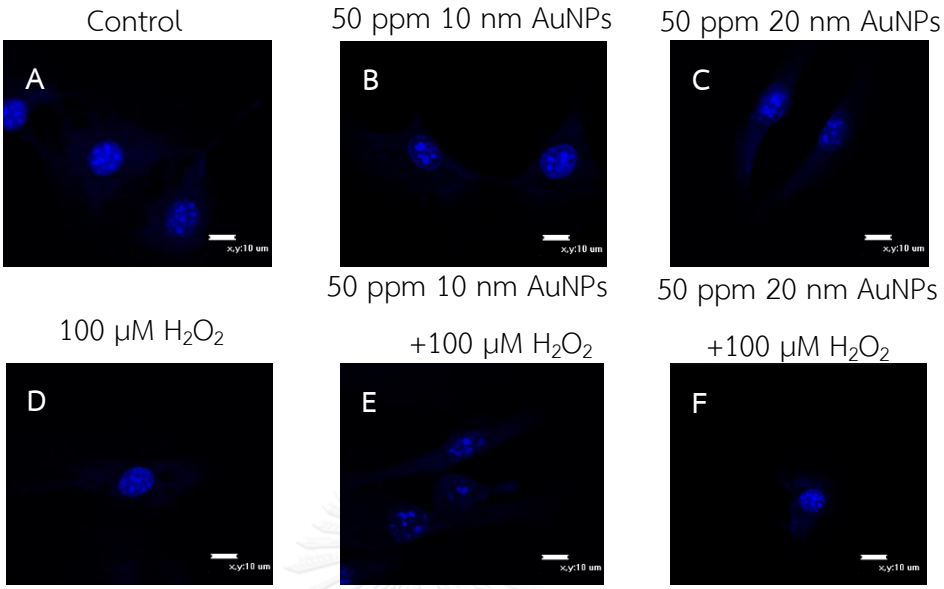

Figure 6. Senescence-association heterochromatin foci of 3T3-L1 after treatment and pretreatment by 10 and 20 nm AuNPs at concentration of 50 ppm, 1000× magnification used.

Fibroblast (NIH 3T3)

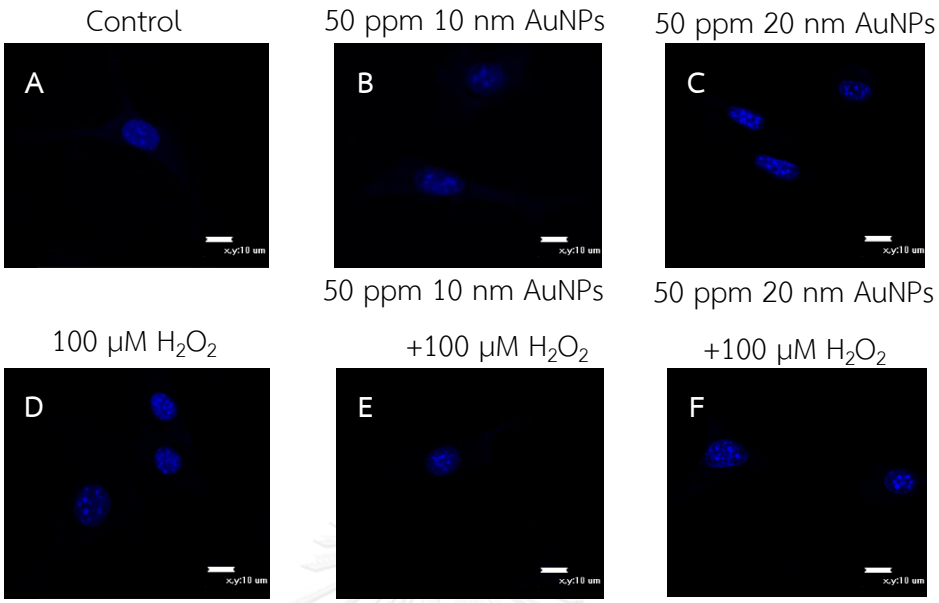

Figure 7. Senescence-association heterochromatin foci of NIH 3T3 after treatment and pretreatment by 10 and 20 nm AuNPs at concentration of 50 ppm, 1000× magnification used.

Table 3. Aging phenotypes of preadipocyte (3T3-L1)

Conditions	Expected morphological parameter				
	Flatten cells	**Large cell shape**	**SA-β-gal stain**	**SA-β-gal activity**	**SAHF**
100 μM H_2O_2	change	change	+ve	↑	no change
5 ppm 10 nm AuNPs	no change	no change	-ve	↓	-
50 ppm 10 nm AuNPs	no change	no change	-ve	↓	no change
5 ppm 20 nm AuNPs	no change	no change	-ve	↓	-
50 ppm 20 nm AuNPs + 100 μM H_2O_2	no change	no change	-ve	↓	no change
5 ppm 10 nm AuNPs + 100 μM H_2O_2	no change	no change	-ve	↓	-
50 ppm 10 nm AuNPs + 100 μM H_2O_2	no change	no change	-ve	↓	no change
5 ppm 10 nm AuNPs + 100 μM H_2O_2	no change	no change	-ve	↓	-
50 ppm 20 nm AuNPs +100 μM H_2O_2	no change	no change	-ve	↓	no change

* ns = Non significance

+ve = Positive

-ve = Negative

\- = Non using for test

↑ = Increase

↓ = Decrease

Table 4. Aging phenotypes of fibroblast (NIH 3T3)

Conditions	Expected morphological parameter				
	Flatten cells	**Large cell shape**	**SA-β-gal stain**	**SA-β-gal activity**	**SAHF**
100 μM H_2O_2	change	change	+ve	↑	no change
5 ppm 10 nm AuNPs	no change	no change	-ve	ns	-
50 ppm 10 nm AuNPs	change	change	+ve	↑	no change
5 ppm 20 nm AuNPs	change	change	+ve	↑	-
50 ppm 20 nm AuNPs + 100 μM H_2O_2	change	change	+ve	↑	no change
5 ppm 10 nm AuNPs + 100 μM H_2O_2	change	change	+ve	ns	-
50 ppm 10 nm AuNPs + 100 μM H_2O_2	change	change	+ve	ns	no change
5 ppm 10 nm AuNPs + 100 μM H_2O_2	change	change	+ve	ns	-
50 ppm 20 nm AuNPs +100 μM H_2O_2	change	change	+ve	ns	no change

* ns = Non significance

+ve = Positive

-ve = Negative

\- = Non using for test

↑ = Increase

↓ = Decrease

Reactive oxygen species (ROS) generation

To show the effect of AuNPs on ROS generation of 3T3-L1 and NIH 3T3 cell lines. ROS generation was measured by H_2DCF-DA assay. Percentage of ROS generation of 3T3-L1 and NIH 3T3 cells treated by AuNPs are shown in Figure 5. Cells were treated by 10 and 20 nm AuNPs at concentrations of 5 and 50 ppm for 1 and 24 h. 1% H_2O_2 was used as a positive control.

In 3T3-L1 cells, ROS generation was significantly decreased after treatment of cells by 50 ppm 10 nm AuNPs and 50 ppm 20 nm AuNPs for 1 h when it was compared to control group (Figure 8A). Compared with control group, ROS generation was not significantly different after treatment of cells by 10 and 20 nm AuNPs in both of concentration of treated AuNPs for 24 h (Figure 8B).

In NIH 3T3 cells, ROS generation was significantly decreased after treatment of cells by 10 nm AuNPs at concentrations of 50 ppm for 1 h when it was compared to control group (Figure 8C) and also significantly decreased after treatment of cells by 5 and 50 ppm 20 nm AuNPs for 24 h when it was compared to control group (Figure 8D).

Preadipocyte (3T3-L1)

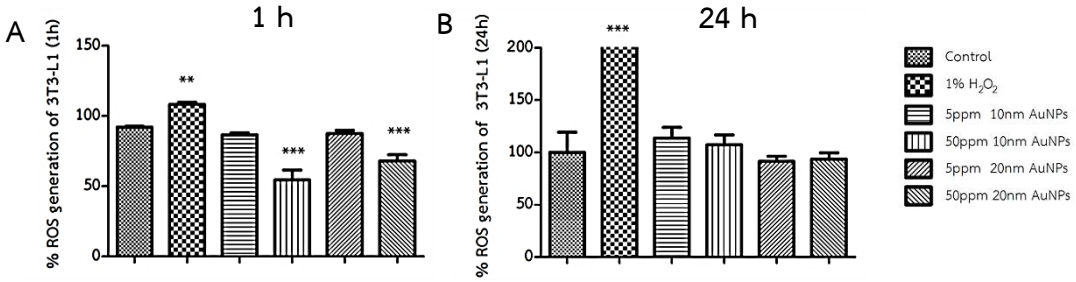

Fibroblast (NIH 3T3)

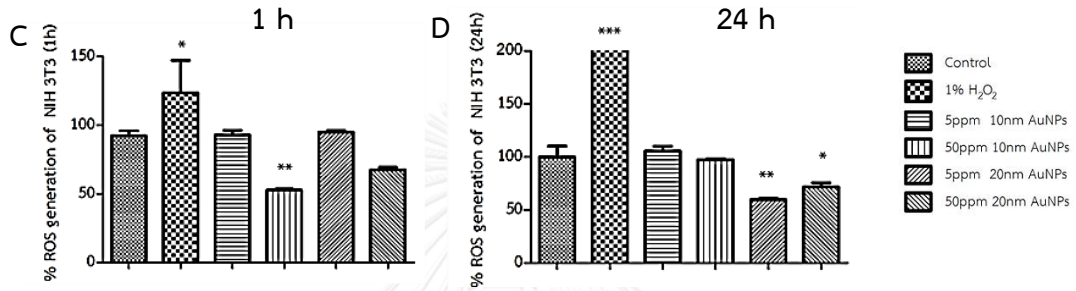

Figure 8. Reactive oxygen species generation of 3T3-L1 and NIH 3T3 cells after exposure to AuNPs for 1 and 24 h. Percentage of ROS in 3T3-L1 (A) and NIH 3T3 (C) cells after exposure to AuNPs at 1 h. Percentage of ROS in 3T3-L1 (B) and NIH 3T3 (D) cells after exposure to AuNPs at 24 h. * indicates that differences are significantly compared with control group. Values are mean ± SD (n=3) significance indicated by: * $p<0.05$, ** $p<0.01$ and *** $p<0.001$

SIRT1, p53, p21, and p16 expression

To show the effect of AuNPs on SIRT1, p53, p21 and p16 mRNA expression of 3T3-L1 and NIH 3T3 cell lines. Relative of SIRT1, p53, p21, and p16 mRNA expression of 3T3-L1 and NIH 3T3 cells treated by AuNPs are shown in Figure 6. Cells were treated and pre-treated by 10 and 20 nm AuNPs at concentrations of 5 and 50 ppm for 24 h. 100 μM H_2O_2 was used as a positive control. In 3T3-L1 cells,

- SIRT1 expression. Compared to control group, 100 μM H_2O_2-exposed cells significantly decreased for SIRT1 mRNA expression. Cells were significantly increased for SIRT1 mRNA expression after treatment of cells by 10 and 20 nm AuNPs in both of concentration of treated AuNPs for 24 h. Compared to 100 μM H_2O_2 group, cells were significantly increased for SIRT1 mRNA expression after pretreatment of cells by 10 and 20 nm AuNPs in both of concentration of treated AuNPs for 24 h (Figure 9A, 10A).
- p53 mRNA expression. Compared to control group, 100 μM H_2O_2-exposed cells significantly increased for p53 mRNA expression. Cells were significantly increased for p53 mRNA expression after treatment of cells by 10 and 20 nm AuNPs in both of concentration of treated AuNPs for 24 h. Compared to 100 μM H_2O_2 group, cells were significantly increased for p53 mRNA expression after pretreatment of cells by 5 ppm 10 nm AuNPs and 5 and 50 ppm 20 nm AuNPs for 24 h (Figure 9B, 10B).
- p21 mRNA expression. Compared to control group, 100 μM H_2O_2-exposed cells significantly decreased for p21 mRNA expression. Cells were significantly increased for p21 mRNA expression after treatment of cells by 5 ppm 10 nm AuNPs and 5 and 50 ppm 20 nm AuNPs for 24 h and significantly decreased for p21 mRNA expression after treatment of cells by 50 ppm 10 nm AuNPs for 24 h. Compared to 100 μM H_2O_2 group, cells were significantly increased for p21 mRNA expression after pretreatment

of cells by 5 ppm 10 nm AuNPs and 5 and 50 ppm 20 nm AuNPs for 24 h (Figure 9C, 10C).

- p16 mRNA expression. Compared to control group, 100 μM H_2O_2-exposed cells significantly decreased for p16 mRNA expression. Cells were significantly increased for p16 mRNA expression after treatment of cells by 5 ppm 10 nm AuNPs and 5 and 50 ppm 20 nm AuNPs for 24 h and significantly decreased for p16 mRNA expression after treatment of cells by 50 ppm 10 nm AuNPs for 24 h. Compared to 100 μM H_2O_2 group, cells were significantly increased for p16 mRNA expression after pretreatment of cells by 5 ppm 10 nm AuNPs and 5 and 50 ppm 20 nm AuNPs for 24 h (Figure 10D, 10D).

In NIH 3T3 cells,

- SIRT1 expression. Compared to control group, 100 μM H_2O_2-exposed cells did not significantly different for SIRT1 mRNA expression. Cells were significantly increased for SIRT1 mRNA expression after treatment of cells by 5 ppm 10 and 50 ppm 20 nm AuNPs for 24 h and significantly decreased for SIRT1 mRNA expression after treatment of cells by 5 ppm 20 nm AuNPs for 24. Compared to 100 μM H_2O_2 group, cells were significantly increased for SIRT1 mRNA expression after pretreatment of cells by 10 nm AuNPs in both of concentration of treated AuNPs for 24 h (Figure 11A, 12A).

- p53 mRNA expression. Compared to control group, 100 μM H_2O_2-exposed cells significantly increased for p53 mRNA expression. Cells were significantly increased for p53 mRNA expression after treatment of cells by 5 and 50 ppm 10 AuNPs and 50 ppm 20 nm AuNPs for 24 h. Compared to 100 μM H_2O_2 group, cells were significantly increased for p53 mRNA expression after pretreatment of cells by 50 ppm 10 nm AuNPs for 24 h and significantly decreased for p53 mRNA expression after pretreatment of cells by 5 ppm 20 nm AuNPs for 24 h (Figure 11B, 12B).

- p21 mRNA expression. Compared to control group, 100 μM H_2O_2-exposed cells did not significantly different for p21 mRNA expression. Cells were significantly increased for p21 mRNA expression after treatment of cells by 20 nm AuNPs in both of concentration of treated AuNPs for 24 h. Compared to 100 μM H_2O_2 group, cells were significantly increased for p21 mRNA expression after pretreatment of cells by 10 and 20 nm AuNPs in both of concentration of treated AuNPs for 24 h (Figure 11C, 12C).
- p16 mRNA expression. Compared to control group, 100 μM H_2O_2-exposed cells did not significantly different for p16 mRNA expression. Cells were significantly increased for p16 mRNA expression after treatment of cells by 5 ppm 10 nm AuNPs and 5 ppm 20 nm AuNPs for 24 h. Compared to 100 μM H_2O_2 group, cells were significantly increased for p16 mRNA expression after pretreatment of cells by 10 nm AuNPs in both of concentration of treated AuNPs for 24 h and significantly decreased for p16 mRNA expression after pretreatment of cells by 50 ppm 20 nm AuNPs for 24 h (Figure 10D, 10D).

Preadipocyte (3T3-L1)

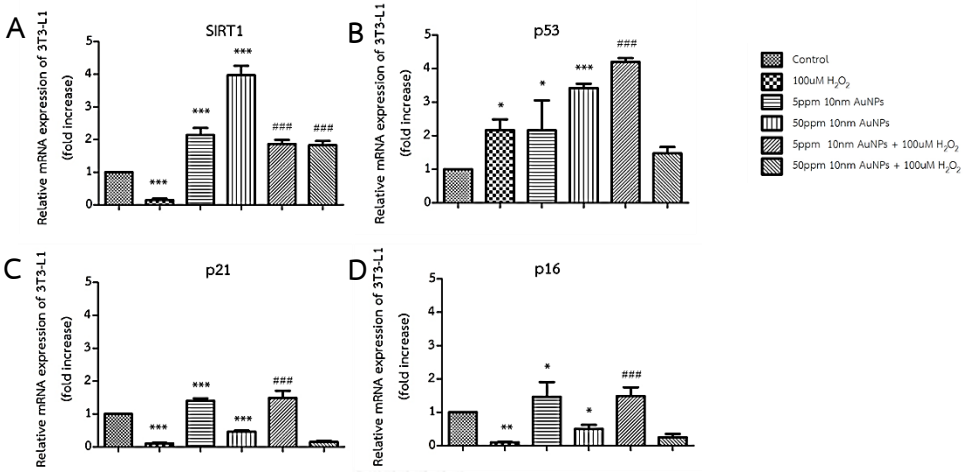

Figure 9. SIRT1, p53, p21, and p16 mRNA expression of 3T3-L1 after treatment and pretreatment by 10 nm AuNPs at concentrations of 5 and 50 ppm. Values are mean ± SD (n=3) significance indicated by: *,# p<0.05, **,## p<0.01 and ***, ### p<0.001.

Preadipocyte (3T3-L1)

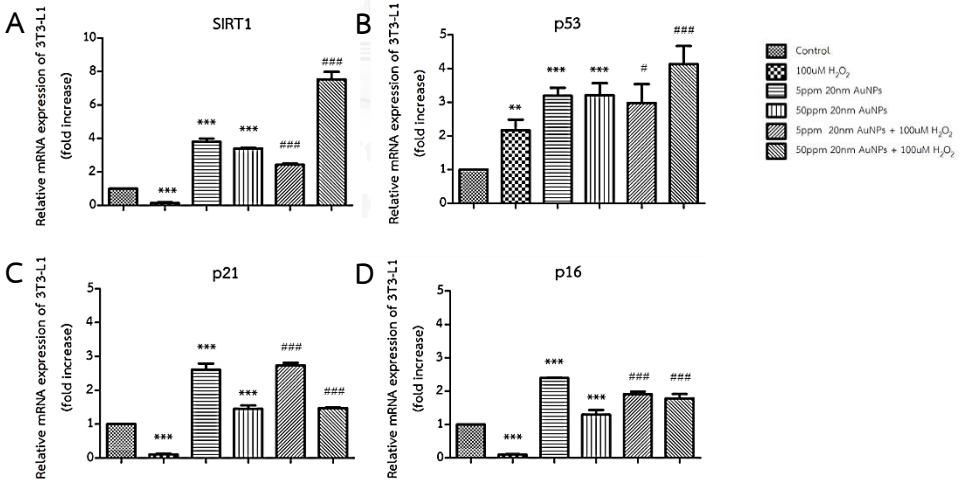

Figure 10. SIRT1, p53, p21, and p16 mRNA expression of 3T3-L1 after treatment and pretreatment by 20 nm AuNPs at concentrations of 5 and 50 ppm. Values are mean ± SD (n=3) significance indicated by: *,# p<0.05, **,## p<0.01 and ***, ### p<0.001.

Fibroblast (NIH 3T3)

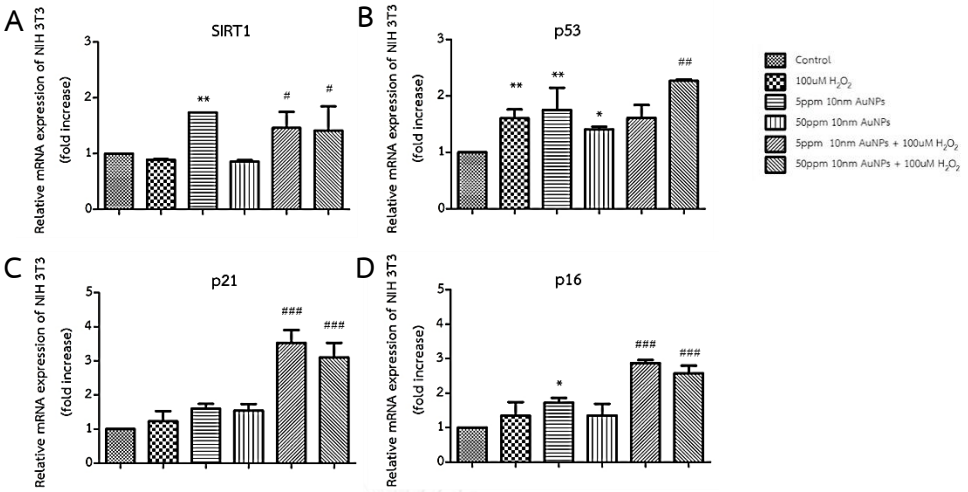

Figure 11. SIRT1, p53, p21, and p16 mRNA expression of NIH 3T3 after treatment and pretreatment by 10 nm AuNPs at concentrations of 5 and 50 ppm. Values are mean ± SD (n=3) significance indicated by: *,# p<0.05, **,## p<0.01 and ***, ### p<0.001.

Fibroblast (NIH 3T3)

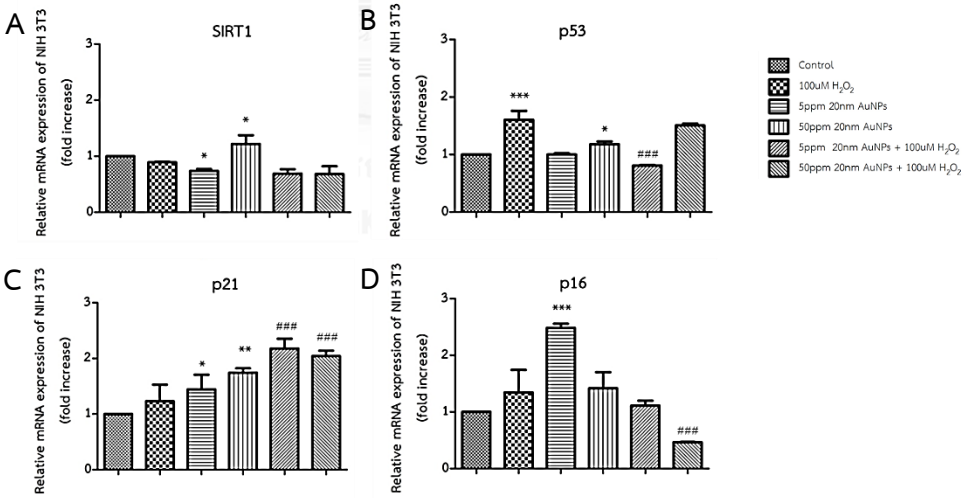

Figure 12. SIRT1, p53, p21, and p16 mRNA expression of NIH 3T3 after treatment and pretreatment by 20 nm AuNPs at concentrations of 5 and 50 ppm. Values are mean ± SD (n=3) significance indicated by: *,# p<0.05, **,## p<0.01 and ***, ### p<0.001.

C/EBPα and PPARγ expression

To show the effect of AuNPs on C/EBPα and PPARγ mRNA expression of 3T3-L1 and NIH 3T3 cell lines. Relative of C/EBPα and PPARγ mRNA expression of 3T3-L1 and NIH 3T3 cells treated by AuNPs are shown in Figure 6. Cells were treated by 10 and 20 nm AuNPs at concentrations of 5 and 50 ppm for 24 h. 100 μM H_2O_2 was used as a positive control.

In 3T3-L1 cells, compared to control group, cells were significantly decreased for C/EBPα and PPARγ mRNA expression after treatment of cells by 10 nm AuNPs in both of concentration of treated AuNPs for 24 h (Figure 13A, 13B). In addition, cells were significantly decreased for C/EBPα and PPARγ mRNA expression after treatment of cells by 20 nm AuNPs in both of concentration of treated AuNPs for 24 h when it was compared to control group (Figure 14A, 14B). Moreover, 50 ppm 20 nm AuNPs group was significantly decreased for PPARγ mRNA expression when it compared to 5 ppm 20 nm AuNPs group.

Preadipocyte (3T3-L1)

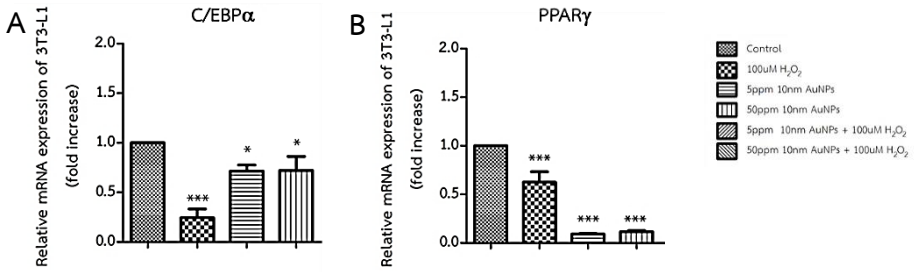

Figure 13. C/EBPα and PPARγ mRNA expression of 3T3-L1 after treatment and pretreatment by 10 nm AuNPs at concentrations of 5 and 50 ppm. Values are mean ± SD (n=3) significance indicated by: *,# p<0.05, **,## p<0.01 and ***, ### p<0.001.

Preadipocyte (3T3-L1)

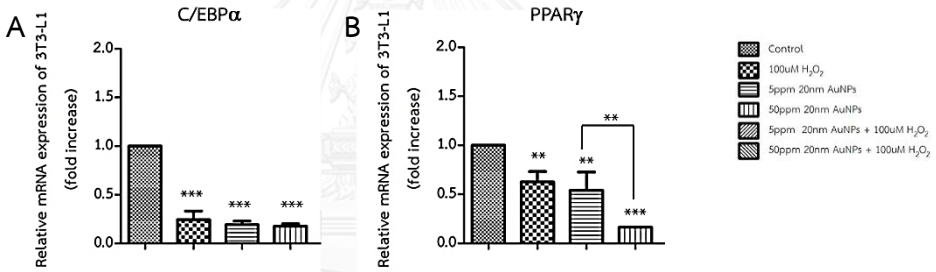

Figure 14. C/EBPα and PPARγ mRNA expression of 3T3-L1 after treatment and pretreatment by 20 nm AuNPs at concentrations of 5 and 50 ppm. Values are mean ± SD (n=3) significance indicated by: *,# p<0.05, **,## p<0.01 and ***, ### p<0.001.

DISCUSSION

Cellular senescence is defined accumulation of cell damage leading to aged-related diseases.[49] There are several factors that caused senescence including intrinsic factors such as genetic instability, telomere attrition, epigenetic alteration, and loss of proteostasis and others while UV irradiation, smoking, drinking, and stress is extrinsic factors.[50] Currently, AuNPs is used more widely in beauty care products.[2] It is still concerned about possible effect on cellular senescence. In this study, preadipocyte (3T3-L1) and fibroblast (NIH 3T3) cell lines use to evaluated cellular senescence change by AuNPs which both cells are found in layer of skin.

Preadipocytes are found in hypodermis layer of skin and one important cells that controlling homeostasis and regulating downstream adipogenic gene have led to generate a new fat cells.[37]

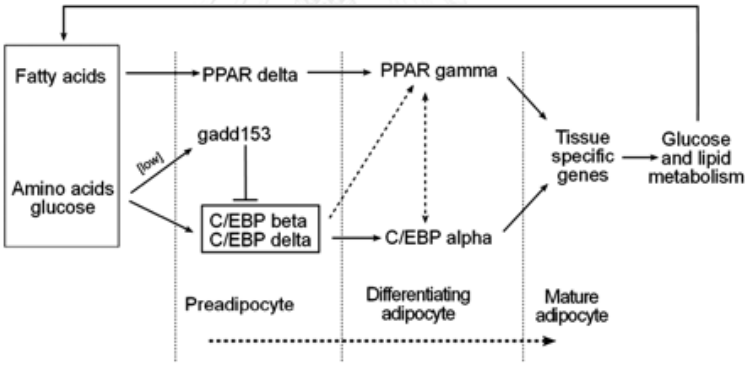

Figure 15. Schematic diagram of differentiating adipocyte by regulation of C/EBPα and PPARγ (modified from reproduction.2005 Oct;130:401-10)

Biologically molecules are related to adipogenesis for instance, peroxisome proliferator-activated receptor-γ (PPARγ) and CCAAT/ enhancer binding protein-α (C/EBPα) were induced by fatty acids, amino acids and glucose for mature adipocyte development (Figure 15).[51] In preadipocyte aging, cells have changed many functions including decreased preadipocyte replication, increased pro-inflammatory cytokine, chemokine, and lipotoxicity.[37] In part of fibroblast, they are found

in dermis layer of skin and have been the most studied in model of skin aging. Fibroblast aging showed connective tissue damage, reduction of new collagen synthesis and decreased collagen and matrix metalloproteinases (MMPs). [38, 52, 53]

In this study, we investigated the effect of AuNPs on cellular senescence change in 3T3-L1 and NIH 3T3 cells. Cell viability was studied to demonstrate the cytotoxicity of AuNPs. Our results showed that AuNP size in 10 nm at concentration of 50 ppm decreased cell viability in both 3T3-L1 and NIH 3T3 cells. In this context, mironava T *et al*. showed cytotoxicity for AuNPs 13 nm at higher concentration on human dermal fibroblast and adipose derived stromal cells (ADSCs).[26, 28] Coradeghini R *et al*. revealed AuNP size in 5 nm at concentration more than 50 μM had cytotoxicity on Balb/3T3 mouse fibroblasts.[27] Aging phenotypes in terms of cellular morphology, SA-β-gal activity, and SAHF were studied to certify the senescent cells which this study found that SA-β-gal activity can be detected early onset from 72 h. Our results showed pretreatment by AuNPs sizes in 10 and 20 nm in both of concentration of treated AuNPs, 3T3-L1 cells were unchangeable to cellular morphology and SAHF. SA-β-gal activity was also decreased after AuNP-pretreated. However, pretreatment by AuNPs revealed extended, flattened, enlarged nuclei, and unchangeable to SAHF in NIH 3T3 cells. Obviously, SA-β-gal activity would be changed more rapidly than cellular morphology and SAHF. On the other hands, cellular morphology and SAHF would have later change in cellular senescent. Our finding showed that AuNPs influence in aging phenotypes dependent on size, concentration and exposure time. Our results suggest that 10 and 20 nm AuNPs at concentrations of 5 ppm and 50 ppm might not effect on intracellular structural proteins and aging phenotypes in 3T3-L1 cells and effect on intracellular structural proteins in NIH 3T3. Furthermore, our result found unchangeable to SAHF in both 3T3-L1 and NIH 3T3 cells. We suggest that epigenetic change might occur slowly in these cells.[54]

To confirm the mechanism of cellular senescence by exposure to AuNPs, high level of ROS can causes a cellular damage and aging.[32] Therefore, ROS generation was studied to demonstrate that cells might be stress from AuNPs. Our results showed that 10 and 20 nm AuNPs in both of concentration of treated AuNPs did not induce ROS generation in 3T3-L1 and NIH 3T3 cells. However, we found that level of ROS was decreased after exposure to 10 nm AuNPs at concentration of 50 ppm. These data confirmed the cell viability results. AuNPs size in 10 nm at concentration 50 ppm cause cytotoxicity leading to cell death and decreasing of ROS levels. Furthermore, these data suggest that AuNPs do not affect oxidative stress based on exposure cell type specific. This work in accordance with previous studies reported that AuNPs size in 15 nm decreased ROS levels in the triple cell co-culture.[55] AuNPs size 10 nm did not show oxidative stress in rat's lungs and heart.[56] Thus, we summarize that cells responded to ROS generation-independent cellular senescence in these cells.

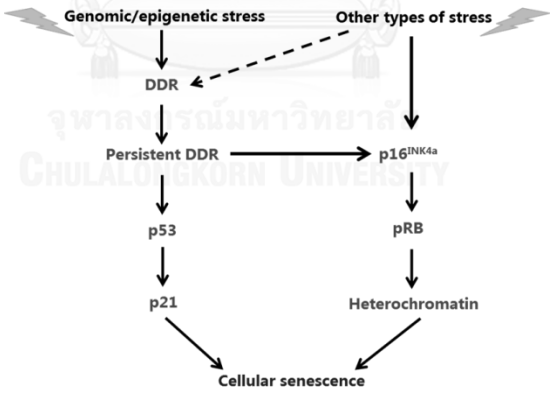

Figure 16. Schematic diagram of p53 pathway in cellular senescence (modified from annual review of physiology. 2013; 75: 685–705)

Oxidative stress-induced cells can lead to cellular senescence through p53 pathway (Figure 16).[32] p53 have been link to up-regulate p21 which is cyclin-kinase inhibitor and downstream target of p53 in cell cycle arrest. Increased p53, p21 and p16 activity promote senescence and shorten life span.[38] We focus on SIRT1

mRNA expression, its activities delay aging[39], p53 pathway of cellular senescence, and mRNA expression of C/EBPα and PPARγ. In most cases, treatment and pretreatment of cells by 10 and 20 nm AuNPs revealed up-regulation of SIRT1 mRNA expression and also up-regulation of p53 and p21 mRNA expression in 3T3-L1 cells. We suggest that up-regulation of p53 mRNA expression cause by SIRT1 by JNK1 specifically deacetylated histone H3 but not p53.[57] Previous studied found that AuNPs size in 15 nm increased p53 mRNA expression in drosophila melanogaster.[58] p53 was over-expressed in response to DNA damage, cellular senescence, apoptosis and preventing cancer development.[31] We also investigated the mRNA expression of C/EBPα and PPARγ, Our results showed that AuNP sizes in10 and 20 nm showed down-regulation of C/EBPα and PPARγ mRNA expression in 3T3-L1 cells. This finding is consistent with previous studies that AuNPs size in 13 and 45 nm reduced adipogenesis and adiponectin secretion.[28]

Although AuNPs have the advantage for aging reduction in preadipocytes but not in fibroblasts, there have been still some limitations in the research that should be addressed. Future study should evaluate AuNPs impact in other controlling mechanism of cellular senescence, and prove whether different size, concentration and exposure time of more than 24 h of treated AuNPs are capable aging reduction and lifespan elongation. Moreover, should be studied *in vivo* model for treatment of AuNPs. In this study, we used only citrate stabilizer and two sizes and concentrations of AuNPs for evaluation of the effect of AuNPs on cellular senescence. Further studies are needed to use AuNPs other size, shape, concentration, or chemical stabilizer which it will have an effect on cellular senescence.

CHAPTER V
CONCLUSION

In conclusion, we report the effect of AuNPs on cellular senescence in preadipocyte (3T3-L1) and fibroblast (NIH 3T3) cell lines. Our findings, AuNPs-exposed cells are able to reduce aging depend on cell-types specific. AuNPs size in 10 nm at concentration 50 ppm had cytotoxicity in both of cells. In part of aging phenotypes, 3T3-L1 cells presented unchangeable cellular morphology, SAHF and decreasing of SA-β-gal activity after exposure to AuNPs. In contrast, NIH 3T3 presented cellular morphological aging, unchangeable of SAHF, and increasing of SA-β-gal activity. Both 3T3-L1 and NIH 3T3 cells did show ROS level change. These data suggest that cells responded to ROS generation-independent cellular senescence. SIRT1 and p53 mRNA expression were up-regulated in 3T3-L1 cells after exposure to AuNPs. Furthermore, C/EBPα and PPARγ expression were down-regulated in 3T3-L1 cells. Based on this knowledge, AuNPs may delay aging process and reduce adipogenesis in 3T3-L1 cells but not delay aging process in NIH 3T3 cells. Thus, the appropriate size and concentration of AuNPs can be selected to apply for cosmeceuticals and anti-aging products.

REFERENCES

1. Kim BYS, Rutka JT, Chan WCW. Nanomedicine. New england journal of medicine. 2010;363:2434-43.

2. Golubovic-Liakopoulos N, Simon SR, Shah B. Nanotechnology use with cosmeceuticals. Seminars in cutaneous medicine and surgery. 2011;30:176-80.

3. Jain KK. Nanomedicine: application of nanobiotechnology in medical practice. Medical principles and practice : international journal of the Kuwait University, health science centre. 2008;17:89-101.

4. Lohani A, Verma A, Joshi H, Yadav N, Karki N. Nanotechnology-based cosmeceuticals. ISRN dermatology. 2014;2014:843687.

5. Zhou J, Ralston J, Sedev R, Beattie DA. Functionalized gold nanoparticles: synthesis, structure and colloid stability. Journal of colloid and interface science. 2009;331:251-62.

6. Alkilany AM, Murphy CJ. Toxicity and cellular uptake of gold nanoparticles: what we have learned so far? Journal of nanoparticle research. 2010;12:2313-33.

7. Shukla R, Bansal V, Chaudhary M, Basu A, Bhonde RR, Sastry M. Biocompatibility of gold nanoparticles and their endocytotic fate inside the cellular compartment: A microscopic overview. 2005;21:10644-54.

8. Negahdary M, Chelongar R, Zadeh SK, Ajdary M. The antioxidant effects of silver, gold, and zinc oxide nanoparticles on male mice in in vivo condition. Advanced biomedical research. 2015;4:69.

9. López-Otín C, Blasco MA, Partridge L, Serrano M, Kroemer G. The hallmarks of aging. Cell. 2013;153:1194-217.

10. Collado M, Blasco MA, Serrano M. Cellular senescence in cancer and aging. Cell. 2007;130:223-33.

11. Kuilman T, Michaloglou C, Mooi WJ, Peeper DS. The essence of senescence. Genes & development. 2010;24:2463-79.

12. Toussaint O, Remacle J, Dumont P, Dierick J-F, Pascal T, Frippiat C, et al. Oxidative stress-induced cellular senescence. eLS: John Wiley & Sons, Ltd; 2001.

13. Wang Z, Wei D, Xiao H. Methods of cellular senescence induction using oxidative stress. Methods in molecular biology. 2013;1048:135-44.

14. Salminen A, Kaarniranta K, Kauppinen A. Crosstalk between oxidative stress and SIRT1: Impact on the aging process. International journal of molecular sciences. 2013;14:3834-59.

15. Vaziri H, Dessain SK, Eagon EN, Imai SI, Frye RA, Pandita TK, et al. hSIR2(SIRT1) functions as an NAD-dependent p53 deacetylase. Cell. 2001;107:149-59.

16. Roco MC. Nanotechnology: convergence with modern biology and medicine. Current opinion in biotechnology. 2003;14:337-46.

17. Vance ME, Kuiken T, Vejerano EP, McGinnis SP, Hochella MF, Jr., Rejeski D, et al. Nanotechnology in the real world: Redeveloping the nanomaterial consumer products inventory. Beilstein journal of nanotechnology. 2015;6:1769-80.

18. Kim JH, Hong CO, Koo YC, Choi HD, Lee KW. Anti-glycation effect of gold nanoparticles on collagen. Biological & pharmaceutical bulletin. 2012;35:260-4.

19. Balasubramanian SK, Jittiwat J, Manikandan J, Ong CN, Yu LE, Ong WY. Biodistribution of gold nanoparticles and gene expression changes in the liver and spleen after intravenous administration in rats. Biomaterials. 2010;31:2034-42.

20. Fathi-Azarbayjani A, Qun L, Chan YW, Chan SY. Novel vitamin and gold-loaded nanofiber facial mask for topical delivery. Journal of the american association of pharmaceutical scientists. 2010;11:1164-70.

21. Sonavane G, Tomoda K, Sano A, Ohshima H, Terada H, Makino K. In vitro permeation of gold nanoparticles through rat skin and rat intestine: effect of particle size. Colloids and surfaces B, biointerfaces. 2008;65:1-10.

22. Pernodet N, Fang X, Sun Y, Bakhtina A, Ramakrishnan A, Sokolov J, et al. Adverse effects of citrate/gold nanoparticles on human dermal fibroblasts. Small journal. 2006;2:766-73.

23. Li JJ, Zou L, Hartono D, Ong CN, Bay BH, Yung LYL. Gold nanoparticles induce oxidative damage in lung fibroblasts in vitro. Advanced materials. 2008;20:138.

24. Qu Y, Lu X. Aqueous synthesis of gold nanoparticles and their cytotoxicity in human dermal fibroblasts-fetal. Biomedical materials. 2009;4:025007.

25. Lu S, Xia D, Huang G, Jing H, Wang Y, Gu H. Concentration effect of gold nanoparticles on proliferation of keratinocytes. Colloids and surfaces B, Biointerfaces. 2010;81:406-11.

26. Mironava T, Hadjiargyrou M, Simon M, Jurukovski V, Rafailovich MH. Gold nanoparticles cellular toxicity and recovery: Effect of size, concentration and exposure time. Nanotoxicology. 2010;4:120-37.

27. Coradeghini R, Gioria S, Garcia CP, Nativo P, Franchini F, Gilliland D, et al. Size-dependent toxicity and cell interaction mechanisms of gold nanoparticles on mouse fibroblasts. Toxicology Letters. 2013;217:205-16.

28. Mironava T, Hadjiargyrou M, Simon M, Rafailovich MH. Gold nanoparticles cellular toxicity and recovery: adipose derived stromal cells. Nanotoxicology. 2014;8:189-201.

29. Hayflick L, Moorhead PS. The serial cultivation of human diploid cell strains. Experimental cell research. 1961;25:585-621.

30. Hayflick L. The limited in vitro lifetime of human diploid cell strains. Experimental cell research. 1965;37:614-36.

31. Liu DP, Xu Y. p53, oxidative stress, and aging. Antioxidants & redox signaling. 2011;15:1669-78.

32. Campisi J. Aging, cellular senescence, and cancer. Annual review of physiology. 2013;75:685-705.

33. Ray PD, Huang B-W, Tsuji Y. Reactive oxygen species (ROS) homeostasis and redox regulation in cellular signaling. Cellular signalling. 2012;24:981-90.

34. Montpetit AJ, Alhareeri AA, Montpetit M, Starkweather AR, Elmore LW, Filler K, et al. Telomere length: A review of methods for measurement. Nursing research. 2014;63:289-99.

35. Kurz DJ, Decary S, Hong Y, Erusalimsky JD. Senescence-associated beta-galactosidase reflects an increase in lysosomal mass during replicative ageing of human endothelial cells. Journal of cell science. 2000;113:3613-22.

36. Luo J, Nikolaev AY, Imai S, Chen D, Su F, Shiloh A, et al. Negative control of p53 by Sir2alpha promotes cell survival under stress. Cell. 2001;107:137-48.

37. Tchkonia T, Morbeck DE, Von Zglinicki T, Van Deursen J, Lustgarten J, Scrable H, et al. Fat tissue, aging, and cellular senescence. Aging cell. 2010;9(5):667-84.

38. Toussaint O, Medrano EE, von Zglinicki T. Cellular and molecular mechanisms of stress-induced premature senescence (SIPS) of human diploid fibroblasts and melanocytes. Experimental gerontology. 2000;35:927-45.

39. Langley E, Pearson M, Faretta M, Bauer U-M, Frye RA, Minucci S, et al. Human SIR2 deacetylates p53 and antagonizes PML/p53-induced cellular senescence. The EMBO Journal. 2002;21:2383-96.

40. Munro J, Barr NI, Ireland H, Morrison V, Parkinson EK. Histone deacetylase inhibitors induce a senescence-like state in human cells by a p16-dependent mechanism that is independent of a mitotic clock. Experimental cell research. 2004;295:525-38.

41. Mirzayans R, Andrais B, Scott A, Paterson MC, Murray D. Single-cell analysis of p16(INK4a) and p21(WAF1) expression suggests distinct mechanisms of senescence in normal human and Li-fraumeni syndrome fibroblasts. Journal of cellular physiology. 2010;223:57-67.

42. Monickaraj F, Aravind S, Nandhini P, Prabu P, Sathishkumar C, Mohan V, et al. Accelerated fat cell aging links oxidative stress and insulin resistance in adipocytes. Journal of biosciences. 2013;38:113-22.

43. Kilic U, Gok O, Erenberk U, Dundaroz MR, Torun E, Kucukardali Y, et al. A remarkable age-related increase in SIRT1 protein expression against oxidative stress in elderly: SIRT1 gene variants and longevity in human. Plos One. 2015;10:e0117954.

44. Dimri GP, Lee XH, Basile G, Acosta M, Scott C, Roskelley C, et al. A biomarker that identifies senescent human cells in culture and in aging skin in vivo. Proceedings of the national academy of sciences of the United States of America. 1995;92:9363-7.

45. Zhang J, Xu E, Ren C, Yan W, Zhang M, Chen M, et al. Mice deficient in Rbm38, a target of the p53 family, are susceptible to accelerated aging and spontaneous tumors. Proceedings of the national academy of sciences of the United States of America. 2014;111:18637-42.

46. Kotas ME, Gorecki MC, Gillum MP. Sirtuin-1 is a nutrient-dependent modulator of inflammation. Adipocyte. 2013;2:113-8.

47. Huang C, Zhang Y, Gong Z, Sheng X, Li Z, Zhang W, et al. Berberine inhibits 3T3-L1 adipocyte differentiation through the PPARgamma pathway. Biochemical and biophysical research communications. 2006;348:571-8.

48. Rose JA, Rabenold JJ, Parast MM, Milstone DS, Abrahams VM, Riley JK. Peptidoglycan Induces necrosis and regulates cytokine production in murine trophoblast stem cells. American journal of reproductive immunology. 2011;66:209-22.

49. Burton DGA. Cellular senescence, ageing and disease. Age. 2009;31(1):1-9.

50. Rattan SIS. Aging is not a disease: Implications for Intervention. Aging and Disease. 2014;5:196-202.

51. Maloney CA, Rees WD. Gene-nutrient interactions during fetal development. Reproduction. 2005;130:401-10.

52. Fligiel SEG, Varani J, Datta SC, Kang S, Fisher GJ, Voorhees JJ. Collagen degradation in aged/photodamaged skin in vivo and after exposure to matrix metalloproteinase-1 in vitro. Journal of investigative dermatology. 2003;120:842-8.

53. Goldstein S. Replicative senescence: the human fibroblast comes of age. Science. 1990;249:1129-33.

54. Jung M, Pfeifer GP. Aging and DNA methylation. BMC Biology. 2015;13:1-8.

55. Brandenberger C, Rothen-Rutishauser B, Muhlfeld C, Schmid O, Ferron GA, Maier KL, et al. Effects and uptake of gold nanoparticles deposited at the air-liquid interface of a human epithelial airway model. Toxicology and applied pharmacology. 2010;242:56-65.

56. Khan HA, Abdelhalim MAK, Al-Ayed MS, Alhomida AS. Effect of gold nanoparticles on glutathione and malondialdehyde levels in liver, lung and heart of rats. Saudi Journal of Biological Sciences. 2012;19:461-4.

57. Nasrin N, Kaushik VK, Fortier E, Wall D, Pearson KJ, de Cabo R, et al. JNK1 phosphorylates SIRT1 and promotes its enzymatic activity. Plos One. 2009;4:e8414.

58. Vecchio G, Galeone A, Brunetti V, Maiorano G, Sabella S, Cingolani R, et al. Concentration-dependent, size-independent toxicity of citrate capped AuNPs in Drosophila melanogaster. Plos One. 2012;7:e29980.

APPENDIX

LIST OF ABBREVIATIONS

ANOVA	Analysis of variance
AuNPs	Gold nanoparticles
cDNA	Complementary DNA
CO_2	Carbon dioxide
C_T	Threshold cycle
C/EBPα	CCAAT/ enhancer binding proteinα
DAPI	4',6-diamidino-2-phenylindole
DMEM	Dulbecco's Modified Eagle Medium
FBS	Fetal bovine serum
GNPs	Gold nanoparticles
H_2DCF-DA	2', 7'-dichlofluorescein-diacetate
$HAuCl_4.3H_2O$	Chloroauric solution
p16, p21, p53	Tumor suppressor gene
PBS	Phosphate buffered saline
PPARγ	Peroxisome proliferator-activated receptorγ
RT-qPCR	Quantitative reverse transcription polymerase chain reaction
ROS	Reactive oxygen species
SA-β-gal	Senescence-associated beta-galactosidase
SAHF	senescence associated heterochromatin foci
SIRT1	SURTUIN1
TEM	Transmission electron microscopy

EQUIPMENT AND CHEMICALS

1. Autoclave (Hirayama, Japan)
2. Biohazard Laminar Flow (Gibco, USA)
3. Cell culture flask 25 cm^2 (Thermo, UK)
4. Cell culture flask 75 cm^2 (Thermo, UK)
5. Centrifuge tube 1.5 mL (Corning, USA)
6. Centrifuge tube 15 mL (Corning, USA)
7. Centrifuge tube 50 mL (Corning, USA)
8. CO_2 incubator (Esco, Singapore)
9. Dulbecco's Modified Eagle's Medium (Sigma, USA)
10. Fetal Bovine Serum (Gibco, USA)
11. Filter Tip (Corning, USA)
12. First strand cDNA synthesis kit (Roche®) (Thermoscientific, USA)
13. Fluorescent microscope (Nikon, Japan)
14. Gold nanoparticles 10 nm (Sigma, USA)
15. H_2DCFDA (Invitrogen, USA)
16. Laboratory balance (Denver instrument, Germany)
17. Malvern Zetasizer Nano Series (Malvern Instrument, England)
18. Microcentrifuge (Hettich, Germany)
19. Phase contrast inverted microscope (Nikon, Japan)
20. pH meter (Denver instrument, Germany)
21. PrestoBlue™ Cell viability Reagent (Invitrogen, USA)
22. pH meter (Denver instrument, Germany)
23. 6-well plate (Corning, USA)
24. 12-well plate (Corning, USA)
25. 24-well plate (Corning, USA)

26. 96-well plate (Corning, USA)
27. 96-black well plate (Corning, USA)
28. Shaker incubator (Heidolph, Germany)
29. StepOnePlus Real-Time PCR System (ABI Applied Biosystems)
30. SYBR GreenER qPCR Supermix Universal (Invitrogen, USA)
31. TRIzol reagent (Invitrogen, USA)
32. Transmission Electron Microscope (Hitachi, Japan)
33. Varioskan Flash microplate reader (Thermo, England)
34. Vortex mixer (Scientific industries, USA)
35. Water bath (Memmert, Germany)

CHEMICAL PREPARATIONS

1. Phosphate buffer saline

   Components

KCl	0.2	g
KH_2PO_4	0.2	g
NaCl	8.0	g
Na_2HPO_4	1.15	g

   Methods

   1. Mix all of chemical components
   2. To add DI water to 1,000 mL
   3. To adjust pH to 7.4 with HCl

2. Dulbecco's Modified Eagle's Medium (DMEM)

   Methods

   1. To dissolve 13.4 g of DMEM with 800 mL DI water
   2. To add 3.7 g of Na_2HCO_3
   3. To adjust pH to with HCl
   4. To add DI water to 1,000 mL
   5. To filtrate by 0.2 μM filter and keep as a medium stock
   6. For working medium preparation, add 10% of FBS and 1% antibiotic (Pen-Strep).

3. Cell Viability Assay Protocol

(PrestoBlue™, Invitrogen, USA, Catalog number A13261)

3.1 Cell culture

Materials

1. 96-well plate
2. Cell culture media
3. Micropipetters
4. CO_2 incubator

Methods

- Cells were seeded in 96-well plates at a density of $1x10^3$ to $1x10^4$ cells/well in 100 µL and incubate at 37°C and 5% CO_2 for 12 h.

3.2 Cell viability assay

Materials

1. Unknown sample for toxicity test
2. DMSO (positive control)

Methods

1. To wash cells with PBS
2. To add 90 µL of culture medium for negative control.
3. To add 90 µL of 50% DMSO for positive control.
4. To treat with 90 µL of unknown samples.
5. To incubate at 37°C and 5% CO_2 for 24 or 72 h.
6. To add 10 µL PrestoBlue™ reagents and incubate for 30 min.
7. To Measure fluorescent product at 560 and 590 nm wavelength by using a microplate reader

Reference

Product information sheet: PrestoBlue™ cell viability reagent protocol by invitrogen™

4. Reactive oxygen species (ROS) Generation protocol

(H_2DCFDA, Invitrogen, USA, Catalog number D399)

4.1 Cell culture

Materials

1. 96-black well plate
2. Cell culture media
3. Micropipetters
4. CO_2 incubator

Methods

- Cells are seed in 96-black well plate at a density of $1x10^3$ to $1x10^4$ cells/ well in 100 µL and Incubate at 37°C and 5% CO_2 for 12 h.

4.2 DCFH-DA assay

Materials

Unknown sample for ROS generation test

1% H_2O_2 (positive control)

Methods

1. To wash cells with PBS
2. To add 100 µL of 0.1M H_2DCFDA
3. To incubate at 37°C and 5% CO_2 for 30 min.
4. To wash cells with PBS
5. To add 100 µL of culture medium for control and 1% H_2O_2 for positive control.
7. To treat with 100 µL of unknown samples.
8. To measure fluorescence excitation and emission at 485 and 528 nm wavelength by using microplate reader.

Reference

Product information sheet: H_2DCFDA by Invitrogen™

VITA

Chalermsri Chayutsatid was born in Phuket, Thailand on 6 April, 1991. She graduated with Bachelor Degree of Science (Biotechnology), from Faculty of Science, King Mongkut's Institute of Technology Ladkrabang in 2012. She enrolled in Master Degree of Medical Science, Faculty of Medicine at Chulalongkorn University in 2013.